PERFORMANCE ANALYSIS OF A SOLAR-ASSISTED AIR CONDITIONING SYSTEM IN DIFFERENT CLIMATIC ZONES OF LIBYA

2025
MASTER THESIS
MECHANICAL ENGINEERING

Jamal Basheer Muhammad ALBARTOULI

Thesis Advisor
Assist. Prof. Dr. Abdulrazzak A. Saleh AKROOT

PERFORMANCE ANALYSIS OF A SOLAR-ASSISTED AIR CONDITIONING SYSTEM IN DIFFERENT CLIMATIC ZONES OF LIBYA

Jamal Basheer Muhammad ALBARTOULI

Thesis Advisor
Assist. Prof. Dr. Abdulrazzak Ahmed Saleh AKROOT

T.C.
Karabuk University
Institute of Graduate Programs
Department of Mechanical Engineering
Prepared as
Master Thesis

KARABÜK
May 2025

I certify that in my opinion the thesis submitted by Jamal Basheer Muhammad ALBARTOULI titled "PERFORMANCE ANALYSIS OF A SOLAR-ASSISTED AIR CONDITIONING SYSTEM IN DIFFERENT CLIMATIC ZONES OF LIBYA" is fully adequate in scope and in quality as a thesis for the degree of Master of Science.

Assist. Prof. Dr. Abdulrazzak Ahmed Saleh AKROOT .....

Thesis Advisor, Department of Mechanical Engineering

This thesis is accepted by the examining committee with a unanimous vote in the Department of Mechanical Engineering as a Master of Science thesis. 09/05/2025

Examining Committee Members (Institutions) **Signature**

Chairman : Assist.Prof.Dr. Abdulrazzak A. Saleh AKROOT (KBÜ).....

Member : Prof. Dr. Emrah DENİZ (KBÜ) .....

Member : Assist.Prof.Dr.Hasanain A. ABDUL WAHHAB (UOT) .....

The degree of Master of Science by the thesis submitted is approved by the Administrative Board of the Institute of Graduate Programs, Karabuk University.

Assoc. Prof. Dr. Zeynep ÖZCAN .....

Director of the Institute of Graduate Programs

"I declare that all the information within this thesis has been gathered and presented in accordance with academic regulations and ethical principles and I have according to the requirements of these regulations and principles cited all those which do not originate in this work as well."

Jamal Basheer Muhammad ALBARTOULI

ABSTRACT

Master Thesis

PERFORMANCE ANALYSIS OF A SOLAR-ASSISTED AIR CONDITIONING SYSTEM IN DIFFERENT CLIMATIC ZONES OF LIBYA

Jamal Basheer Muhammad ALBARTOULI

Karabük University
Institute of Graduate Programs
Department of Mechanical Engineering

Thesis Advisor:
Assist. Prof. Dr. Abdulrazzak Ahmed Saleh AKROOT
May 2025, 72 pages

This study delivers a comprehensive thermodynamic and exergy analysis of a solar-powered absorption cooling system tailored for Libya's hot, arid climates—specifically in Tripoli, Benghazi, and Misrata. The system employs Parabolic Trough Collectors (PTC) to harness and store solar energy, which in turn drives a lithium bromide–water ($LiBr–H_2O$) cycle comprising a generator, absorber, evaporator, condenser, solution heat exchanger (SHEX), and circulation pumps. By utilizing abundant solar resources, the design aims to reduce dependence on conventional fossil-fuel-based cooling methods and enhance sustainability in regions with high cooling demands.

Performance metrics are evaluated under varying operational conditions, including alterations in the generator inlet temperature, evaporator temperature, collector area, and Direct Normal Irradiance (DNI). The analysis focuses on the system's coefficient

of performance (COP), exergy efficiency, cooling load, and heat transfer rates, pinpointing optimal conditions for maximum efficiency.

Results indicate that raising the generator inlet temperature increases the cooling load from approximately 5 kW to 10 kW, with a relatively stable COP of around 0.75–0.8. Meanwhile, the exergy efficiency remains near 35%, suggesting limited additional irreversibilities at higher temperatures. Increasing DNI significantly enhances cooling capacity and heat transfer, highlighting the critical role of solar radiation availability. Collector area growth—from 50 m² to 100 m²—correlates directly with higher cooling output (2.5 kW to 14 kW). However, raising the evaporator temperature from –3 °C to 6 °C reduces exergy efficiency from roughly 80% to 32%, though the COP stays largely unchanged.

Overall, the study confirms that each parameter has an optimal operating range, balancing performance, efficiency, and cost. The proposed solar-driven absorption system thus emerges as a practical, eco-friendly alternative to conventional cooling methods in Libya's major cities.

Key Word **:** Solar, Air-conditioning system, Tripoli, Benghazi, Misrata.

Science Code :91441

ÖZET

Yüksek Lisans

LİBYA'NIN FARKLI İKLİM BÖLGELERİNDE GÜNEŞ DESTEKLİ BİR İKLİMLENDİRME SİSTEMİNİN PERFORMANS ANALİZİ

Jamal Basheer Muhammad ALBARTOULI

Karabük Üniversitesi
Lisansüstü Eğitim Enstitüsü
Makine Mühendisliği Anabilim Dalı

Tez Danışmanı:
Dr. Öğr. Üyesi Abdulrazzak Ahmed Saleh AKROOT
Mayıs 2025, 72 sayfa

Bu çalışma, özellikle Trablus, Bingazi ve Misrata olmak üzere Libya'nın sıcak ve kurak iklimleri için özel olarak tasarlanmış, güneş enerjisiyle çalışan bir absorpsiyonlu soğutma sisteminin kapsamlı bir termodinamik ve ekserji analizini sunmaktadır. Sistem, güneş enerjisinden yararlanmak ve depolamak için Parabolik Tekneli Kollektörler (PTC) kullanmakta, bu da bir jeneratör, soğurucu, buharlaştırıcı, kondenser, çözelti ısı eşanjörü (SHEX) ve sirkülasyon pompalarından oluşan bir lityum bromür-su ($LiBr-H_2O$) döngüsünü çalıştırmaktadır. Tasarım, bol güneş kaynaklarını kullanarak geleneksel fosil yakıt bazlı soğutma yöntemlerine bağımlılığı azaltmayı ve yüksek soğutma talepleri olan bölgelerde sürdürülebilirliği artırmayı amaçlamaktadır.

Performans ölçütleri, jeneratör giriş sıcaklığı, buharlaştırıcı sıcaklığı, kolektör alanı ve Doğrudan Normal Işınım (DNI) değişiklikleri dahil olmak üzere değişen çalışma koşulları altında değerlendirilmiştir. Analiz, sistemin performans katsayısına (COP), ekserji verimliliğine, soğutma yüküne ve ısı transfer oranlarına odaklanarak maksimum verimlilik için en uygun koşulları belirlemektedir.

Sonuçlar, jeneratör giriş sıcaklığının yükseltilmesinin soğutma yükünü yaklaşık 5 kW'tan 10 kW'a çıkardığını ve COP'nin 0,75-0,8 civarında nispeten istikrarlı olduğunu göstermektedir. Bu arada, ekserji verimliliği %35 civarında kalarak daha yüksek sıcaklıklarda sınırlı ek tersinmezliklere işaret etmektedir. DNI'nin artırılması, soğutma kapasitesini ve ısı transferini önemli ölçüde artırarak güneş radyasyonunun kullanılabilirliğinin kritik rolünü vurgulamaktadır. Kollektör alanının 50 m²'den 100 m²'ye çıkarılması, daha yüksek soğutma çıktısıyla (2,5 kW'tan 14 kW'a) doğrudan ilişkilidir. Ancak buharlaştırıcı sıcaklığının -3 °C'den 6 °C'ye yükseltilmesi, ekserji verimliliğini kabaca %80'den %32'ye düşürse de COP büyük ölçüde değişmiyor.

Genel olarak çalışma, her bir parametrenin performans, verimlilik ve maliyeti dengeleyen optimum bir çalışma aralığına sahip olduğunu doğrulamaktadır. Önerilen güneş enerjili absorpsiyon sistemi böylece Libya'nın büyük şehirlerinde geleneksel soğutma yöntemlerine pratik, çevre dostu bir alternatif olarak ortaya çıkmaktadır.

Anahtar Sözcükler : Güneş, İklimlendirme sistemi, Trablus, Bingazi, Misrata.

Bilim Kodu **:** 91441

ACKNOWLEDGMENT

Praise be to God, who has granted me the strength and perseverance to complete this research, and may it benefit students, researchers, and the broader scientific community in the future.

I would like to express my sincere and profound gratitude to my supervisor, Assist. Prof. Dr. Abdulrazak Ahmed Saleh AKROUT.

I extend my sincere thanks to my colleagues and friends at Karabük University for their cooperation, support, and camaraderie. The academic discussions and moments of shared learning have greatly enriched my experience and contributed to my personal and professional growth.

I also extend my sincere appreciation to the administrative staff at Karabük University—the Graduate Programs Institute and the Department of Mechanical Engineering—for their professionalism and assistance in ensuring smooth administrative procedures throughout my graduate studies.

To my beloved family, I owe everything. Thank you for instilling in me the values of perseverance and a passion for learning that have endured throughout my life. To my entire family,

This journey has been both challenging and transformative. I reflect on this chapter with deep appreciation for everyone who has supported me. The knowledge gained and the relationships I built will remain a lasting legacy of this academic endeavor.

CONTENTS

Page

Page

LISTS OF FIGURES

Page

Page

LISTS OF TABLES

Page

SYMBOLS AND ABBREVIATIONS

SYMBOLS

A_coll	: collector area (m2)
COP	: coefficient of performance
DNI	: direct normal Irradiations (W/m2)
$\dot{E}$	: exergy (kW)
h	: specific enthalpy (kJ/kg)
$\dot{m}$	: mass flow rate (kg/s)
P	: pressure (kPa)
$\dot{Q}$	: heat transfer (kW)
s	: specific entropy (kJ/kg. K)
T	: temperature (°C)
U	: overall heat transfer coefficient (W/m2.K)
$\dot{W}$	: work done (kW)
ŋ	: efficiency (%)
x	: LiBr concentration

ABBREVIATIONS

Abs	: Absorber
Cond	: Condenser
EV	: Expansion Valve
Evap	: Evaporator
Gen	: Generator
SHES	: Sensible Heat Exchanger
PTC	: Parabolic Trough Collectors
ARC	: Absorption Refrigeration Cycle
HE	: Heat Exchanger
HTF	: Heat Transfer Fluid
P	: Pump
TST	: Thermal Storage Tank

CHAPTER 1

INTRODUCTION

Rising temperatures and ongoing urban growth have steadily pushed the global demand for cooling solutions [1]. Today, air conditioning has become an essential part of modern life, but it has significant implications for energy consumption and environmental sustainability [2]. In regions with high cooling needs, most air conditioners still rely heavily on electricity generated from fossil fuels, leading to increased greenhouse gas emissions and placing substantial strain on energy infrastructures. As a result, researchers and policymakers alike are paying more attention to alternative and renewable energy sources for air conditioning systems [3].

Solar power is a particularly promising choice for running air conditioning systems among the various renewable energy options [4,5]. By tapping into the sun's abundant and renewable energy, solar-assisted cooling offers an efficient way to meet high cooling demands [6]. These systems are especially well-suited to sun-drenched regions like Libya, where elevated solar irradiation levels can be utilized to maximum effect. By integrating photovoltaic and solar thermal technologies into cooling applications, solar-assisted air conditioning can significantly lower energy expenses, boost sustainability, and play a pivotal role in combating climate change.

This research examines how feasible and effective a solar-assisted air conditioning system can be when it uses parabolic trough solar collectors to power an absorption chiller, drawing on case studies from three different climate zones in Libya. The first chapter outlines the core ideas behind human thermal comfort, solar energy, and the integration of solar-powered cooling systems, especially those employing parabolic trough collectors, to deliver sustainable air conditioning solutions.

1.1. HUMAN COMFORT AND AIR CONDITIONING

Modern air conditioning systems are primarily designed to improve comfort since indoor temperature plays a big role in productivity, health, and overall quality of life. However, comfort isn't driven by temperature alone—factors like humidity, air movement, and radiant temperature also come into play [6]. The necessity of maintaining appropriate indoor conditions in residences, commercial establishments, and industrial facilities is widely recognized, as high temperatures can lead to pain, fatigue, and health issues [7]. Attaining thermal comfort in arid and hot regions like Libya is particularly challenging due to persistent high temperatures. These necessitate efficient cooling systems that maintain optimal indoor conditions while minimizing energy consumption and environmental impact [8].

1.1.1. Definition of Thermal Comfort

Humans spend most of their lives indoors, making indoor environmental quality crucial to health, productivity, and general well-being. The American Society of Heating, Refrigerating, and Air-Conditioning Engineers (ASHRAE) defines thermal comfort as "the condition of mind that expresses satisfaction with the thermal environment." This definition emphasizes that comfort is subjective and varies based on metabolism, clothing, activity level, and personal preference [9,10]. However, a broad consensus exists regarding the environmental parameters—namely temperature, humidity, air velocity, and radiant heat exchange—that facilitate a comfort zone for most people [11].

1.1.2. Evolution and Necessity of Air Conditioning

Modern air conditioning (AC) traces its origins to early industrial operations that needed specific humidity levels to maintain product quality. Over time, AC evolved from basic mechanical fans and evaporative coolers into more advanced centralized and decentralized vapor-compression systems. This progress was driven by the need for precise temperature and humidity control, particularly in environments like commercial buildings, hospitals, and data centers [12,13].

In hot regions, AC systems protect people from heat-related health risks such as heat stroke and dehydration. Plus, many modern electronic devices—like servers, medical machines, and lab equipment—depend on AC to prevent overheating. Because of these diverse applications, air conditioning has moved beyond being a luxury and is now considered a necessity, especially in areas with high solar irradiation and elevated temperatures, such as Libya.

1.1.3. Limitations of Conventional AC Systems

Most conventional air conditioning units rely on vapor-compression cycles powered by electricity derived from fossil fuels. These traditional systems pose several challenges [14,15]:

- High Energy Consumption: Cooling demand can constitute over half of a building's electricity usage during peak summer months.
- Environmental Impact: Relying on electricity produced by fossil fuels increases greenhouse gas emissions. The refrigerants used (e.g., hydrofluorocarbons, HFCs) can also have high global warming potentials.
- Strain on Electrical Grids: Surges in cooling demand, particularly on hot days, can lead to power shortages or rolling blackouts in regions with inadequate infrastructure.

Transitioning to solar-assisted or wholly solar-powered cooling systems presents an opportunity to mitigate these limitations by tapping into the abundant solar resources in sunbelt regions, including Libya.

1.2. SOLAR ENERGY

1.2.1. Overview of Solar Energy

Solar energy is one of Earth's most abundant and widely distributed renewable energy sources. The sun emits approximately 173,000 terawatts of energy, significantly

exceeding global energy consumption [16,17]. Employing solar thermal and photovoltaic (PV) technologies to harness even a fraction of this energy would provide sustainable solutions for diverse applications, including air cooling, water heating, and electricity generation [18].

Libya possesses significant solar irradiation due to its geographic location in North Africa. Data from the Libyan Renewable Energy Authority indicates that the country receives an average daily solar radiation of 6–7 kWh/m², rendering it an ideal candidate for solar-assisted cooling systems [19]. Incorporating solar energy into cooling applications presents numerous benefits [20]:

- Utilizing solar energy reduces reliance on conventional power sources, alleviating the national grid's burden.
- Solar cooling systems mitigate emissions, contributing to the deceleration of global warming.
- Despite the higher initial investment, solar cooling reduces operational expenses over time.

1.2.2. Solar Energy Technologies

Common technologies used to harness solar energy include [21]:

- Photovoltaic (PV) Systems: Convert sunlight directly into electricity.
- Solar Thermal Systems: Solar collectors capture thermal energy to heat water and spaces or drive thermodynamic cycles.
- Concentrating Solar Power (CSP) Systems: Focus or concentrate on sunlight to generate high temperatures, which can produce steam for electricity generation or drive other thermodynamic processes (such as in absorption chillers) [22].

1.3. PARABOLIC TROUGH SOLAR COLLECTORS

Parabolic trough solar collectors (PTCs) are among the most frequently utilized and efficient solar thermal devices for capturing and converting solar radiation into thermal energy [23]. Parabolic mirrors in these collectors focus sunlight onto a receiver tube at the parabola's focal point. A heat transfer fluid (HTF), typically a synthetic oil or molten salt, traverses this tube to collect concentrated solar energy, which is then employed for industrial heating, solar-assisted cooling systems, and power generation, among other applications, as seen in Figure 1.1 [24–26].

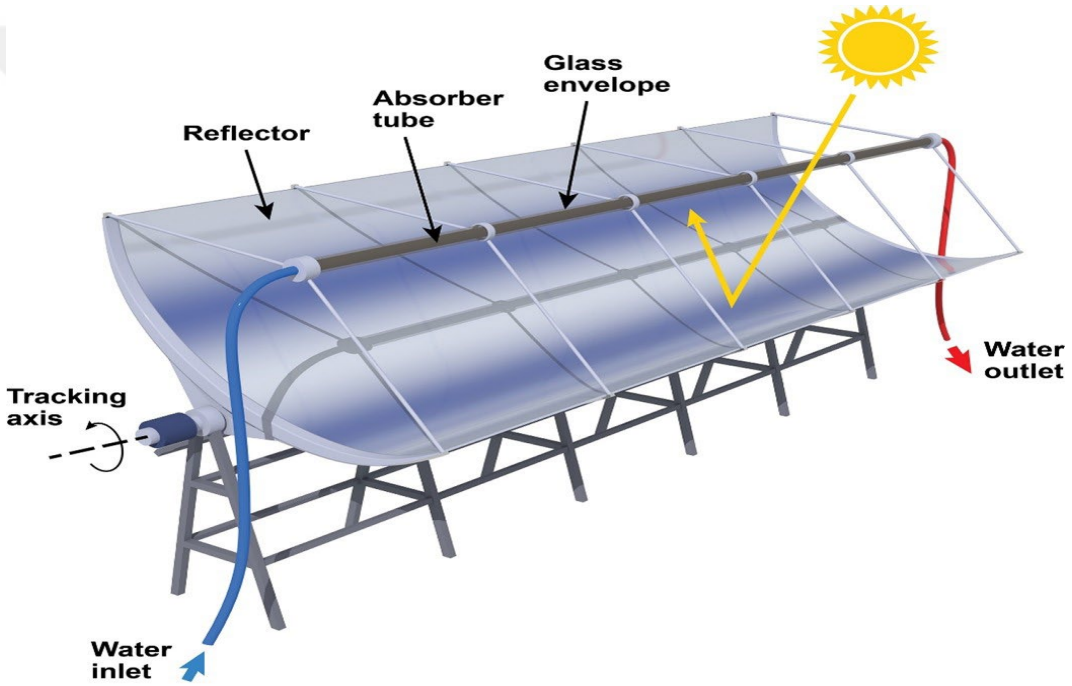

Figure 1.1. Parabolic trough solar collector [27].

A PTC system consists of the following main components [24–26]:

- Reflective Mirror: Typically composed of silvered or aluminized glass that reflects and focuses incoming solar radiation.
- Receiver Tube (Absorber): Positioned at the focus of the parabolic trough. It is often coated with a spectrally selective material to maximize absorption and reduce thermal emissivity.

- Heat Transfer Fluid (HTF): Commonly synthetic oil, pressurized water, or molten salts. This fluid transports the captured heat to a heat exchanger or directly to a thermal application like an absorption chiller.
- Support and Tracking System: Troughs usually track the sun along a single axis (east-west or north-south), ensuring that sunlight remains concentrated on the receiver throughout the day.

PTCs provide numerous advantages and have demonstrated efficacy in harnessing solar energy for high-temperature applications [28,29].

- PTCs can achieve 60% to 75% of thermal efficiencies among the most efficient solar thermal systems.
- Large-scale solar facilities and small-scale industrial applications can benefit from these technologies.
- PTCs have been successfully implemented worldwide, demonstrating long-term operational stability for decades.

PTCs can be integrated with absorption chillers for air conditioning applications, wherein the collected thermal energy propels a cooling cycle. This method provides a sustainable and energy-efficient alternative to conventional electrically powered cooling systems, particularly in warmer regions. These systems are advantageous for reducing peak energy demand and decreasing greenhouse gas emissions, as they significantly diminish electricity use by harnessing solar thermal energy.

1.4. SOLAR-POWERED COOLING SYSTEM

A solar-powered cooling system directly or indirectly uses solar energy to power refrigeration cycles. When solar thermal collectors (like parabolic troughs) are used, the captured heat can drive an absorption or adsorption chiller. Alternatively, photovoltaic (PV) panels can supply electricity to a conventional vapor-compression cycle [26,30]. The core idea is to synchronize cooling demand with solar availability, reducing reliance on grid electricity and diminishing the carbon footprint of air conditioning.

Solar cooling can be broadly categorized by the energy type used to drive the cooling process [31,32]:

- **Thermally Driven Systems**: Use heat from solar thermal collectors to drive a refrigeration cycle (e.g., absorption or adsorption systems).
- **Photovoltaic-Driven Systems**: Solar PV panels power a conventional vapor-compression refrigeration cycle.

Figure 1.2 contrasts two primary techniques of solar-powered cooling. Solar collectors convert sunlight into thermal energy, which is stored and later employed to power an absorption (or adsorption) refrigeration system, as illustrated in the thermally powered cooling cycle diagram on the left. The essential components include an absorber, regenerator, and thermal storage tank, with an evaporator and condenser completing the cycle. The photovoltaic system on the right produces electricity to operate a conventional vapor-compression refrigeration cycle. These figures collectively illustrate the fundamental distinction between the direct utilization of solar heat (left) and the conversion of solar energy into electricity (right) for cooling applications.

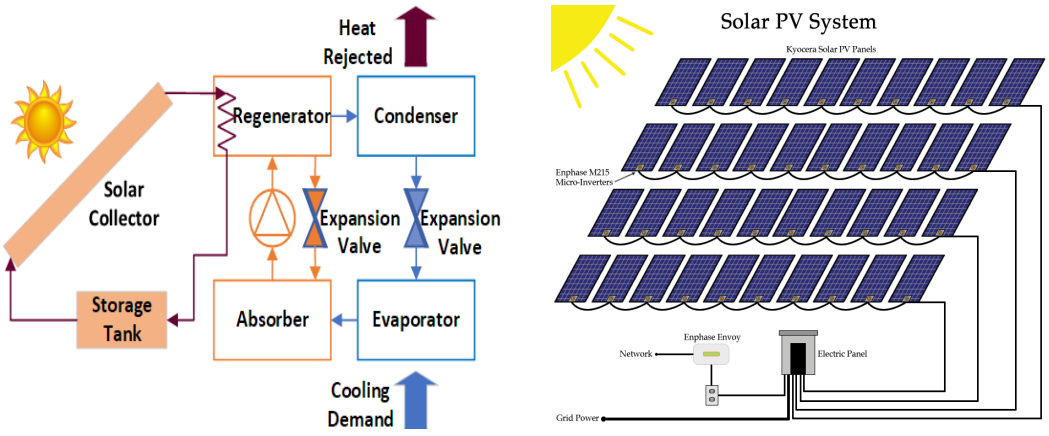

(a) (b)

Figure 1.2. Schematic diagrams of thermally driven and photovoltaic-driven solar cooling systems [31,32].

1.5. ABSORPTION CHILLER

Absorption chillers utilize thermal energy rather than electricity to facilitate the cooling process, serving as an energy-efficient alternative to conventional vapor-compression cooling systems [33,34]. When integrated with solar-assisted cooling systems, these chillers are particularly beneficial since they may utilize the heat generated by solar collectors to supply chilled water for air conditioning applications [35]. Absorption chillers provide an effective solution for continuous cooling in regions with high solar irradiation, such as Libya.

Absorption chillers operate on a thermally driven refrigeration cycle, utilizing a refrigerant-absorbent pair to transfer heat and produce cooling. The two most frequently employed working pairs are [35]:

- The combination of water and lithium bromide is appropriate for air cooling applications, whereby water functions as the refrigerant and lithium bromide serves as the absorbent (H_2O-LiBr).
- Applied industrial refrigeration utilizing ammonium and water (NH_3-H_2O) uses water as the absorbent and ammonia as the refrigerant.

Figure 1.3 illustrates the operational principle of a conventional absorption chiller, featuring a refrigerant (depicted in blue) and an absorbent (shown in red) running via four main components: generator, condenser, evaporator, and absorber. An external heat source, such as waste heat or solar thermal energy—extracts the refrigerant vapor from the "rich" solution in the generator. Subsequently, the high-pressure vapor transitions to the condenser, condensing into liquid and dissipating heat. The refrigerant traverses an expansion valve, undergoes a pressure reduction, and subsequently enters the evaporator, which absorbs heat from the cooling load and reverts to vapor. This low-pressure vapor is ultimately gathered in the absorber and combined with the "poor" absorbent solution to produce heat. A pump and solution exchanger facilitate the return of the enriched ("rich") solution to the generator, thereby completing the cycle.

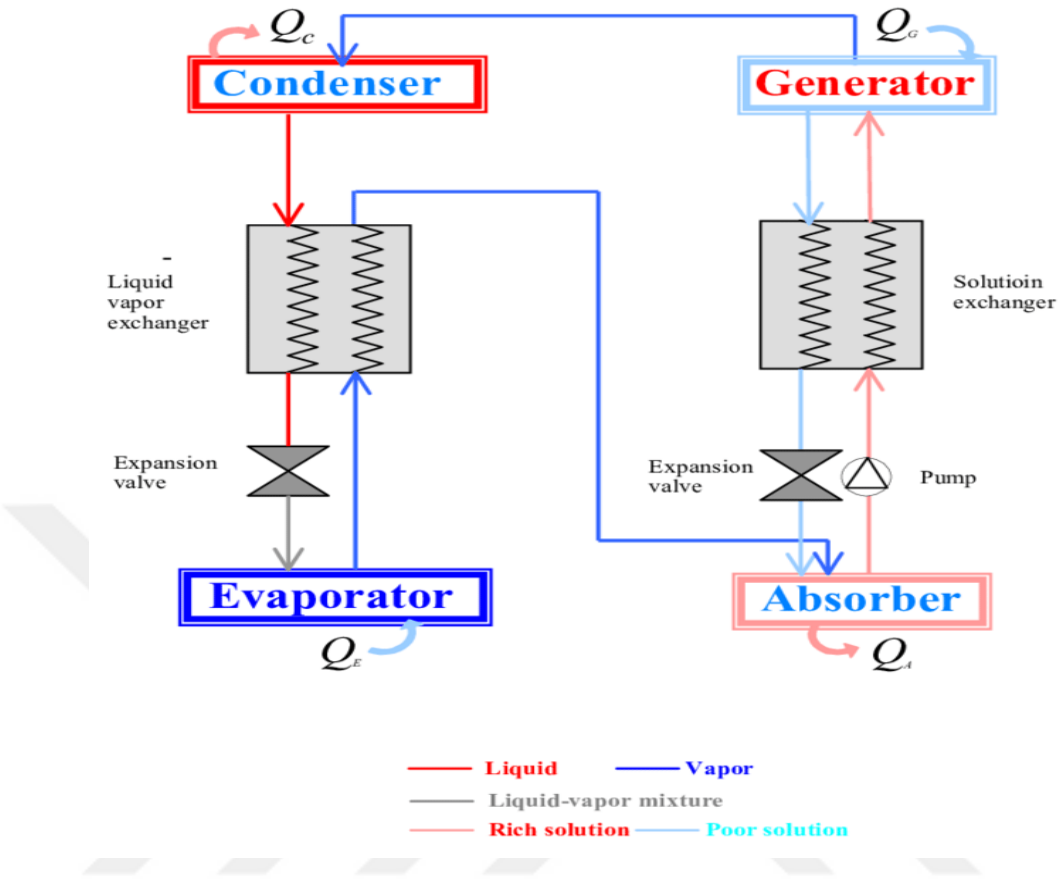

Figure 1.3. Schematic diagrams of absorption chiller [36].

Including absorption chillers with solar thermal systems offers many advantages, including [37]:

- Absorption chillers use thermal energy for operation; hence, unlike conventional air conditioners, they demand very low electrical input.
- Reducing dependence on power helps to cut carbon emissions and lessens the environmental impact of cooling systems.
- Absorption chillers contain fewer moving components than vapor-compression systems, which lowers maintenance costs and increases lifetime.
- Peak load reduction, particularly in areas with high cooling demand, these chillers assist in relieving strain on the power grid by using solar energy during maximum daylight hours.

1.6. WEATHER DATA FOR THREE CITIES IN LIBYA

Weather conditions significantly influence the efficacy and functionality of solar-assisted air conditioning systems. Solar collectors' thermal performance and air conditioning systems' cooling capacity are directly influenced by solar irradiation, ambient temperature, relative humidity, wind speed, longitude, and altitude. Analyzing meteorological data from three prominent Libyan cities—Tripoli, Benghazi, and Misrata—each exhibiting distinct climatic characteristics—facilitates a comprehensive performance evaluation.

1.6.1 Tripoli (Coastal Zone)

- Tripoli, Libya's capital, lies on the Mediterranean coast and experiences a hot-summer Mediterranean climate. Summers are long, extremely hot, and dry, with temperatures often climbing above 35°C during the hottest months. Winters remain mild and somewhat rainy, hovering between 10°C and 18°C on average. Because Tripoli enjoys abundant daily solar radiation—about 6–7 kWh/m²—it's an ideal location for implementing solar energy systems, including solar-assisted air conditioning.
- **Latitude:** 32.8872° N
- Longitude: 13.1913° E
- Elevation: 81 meters above sea level
- Mean Summer Temperature: 30-35°C.
- Solar Irradiance: 6-7 kWh/m² daily.
- Humidity Levels: Moderate, exhibiting seasonal fluctuations

Tripoli's coastal climate makes it especially well-suited for solar cooling systems, thanks to its moderate humidity and abundant sunlight. These conditions create near-perfect circumstances for running solar absorption chillers.

1.6.2 Benghazi (Coastal to Semi-Arid Zone)

Benghazi, located in northeastern Libya, sits at the crossroads between a Mediterranean and a semi-arid climate. Summers are hot with slightly lower humidity than Tripoli, and winters are relatively cool and breezy. Temperatures typically range from 28°C to 38°C in summer and 8°C to 16°C in winter. Although Benghazi's solar radiation is marginally lower than Tripoli's, it still offers substantial sunlight for solar energy projects. Because of its varied climate, Benghazi provides an excellent case study for testing how well solar-assisted air conditioning systems adapt in semi-arid environments.

- **Latitude:** 32.1167° N
- **Longitude:** 20.0667° E
- **Altitude:** 132 m above sea level
- **Average Summer Temperature:** 28-38°C
- **Solar Irradiance**: 5.5-6.5 kWh/m² per day
- **Humidity Levels:** Moderate to low

1.6.3 Misrata (Coastal Zone)

Along the northwestern coast, Misrata has a climate similar to Tripoli's but with slightly greater temperature swings. Summers can reach 37°C, while winters average between 12°C and 20°C. Misrata is an ideal spot for solar-powered initiatives thanks to consistently high solar irradiance. In fact, its strong solar potential and its coastal climate make it a valuable point of reference when assessing the feasibility of solar-assisted cooling in urban seaside regions.

- **Latitude:** 32.3754° N
- **Longitude:** 15.0925° E
- **Altitude:** 34 m above sea level
- **Average Summer Temperature:** 32-37°C
- **Solar Irradiance:** 6.2-7 kWh/m² per day

- **Humidity Levels:** Moderate to high

1.7. PROBLEM STATEMENTS

Despite Libya’s substantial solar energy potential, its hot and arid climate makes it challenging to meet the growing demand for air conditioning. Rising reliance on conventional, fossil-fuel-based cooling has increased electricity consumption, boosted carbon emissions, and strained the national grid. These obstacles underline the critical need for sustainable, energy-efficient solutions that utilize Libya’s abundant solar resources and reduce dependence on traditional power.

Solar-assisted absorption cooling stands out as a promising option, using solar thermal energy to power the cooling process. However, its effectiveness is greatly affected by local meteorological conditions such as humidity, ambient temperature, and solar irradiation. Although Libya offers strong solar potential, little research has focused on how different climates influence the performance of solar absorption cooling systems. Given the country’s diverse climate zones, it’s vital to study how this approach functions in multiple cities—specifically Tripoli, Benghazi, and Misrata—so that we can fully understand and optimize its capabilities across various conditions.

Another big challenge is optimizing the system's running settings. The efficiency of absorption chillers depends on factors like generator inlet temperature, evaporator temperature, and solar collector area. These systems may fail to perform efficiently without proper optimization, leading to increased operational costs and energy losses.

This thesis examines, optimizes, and evaluates the feasibility of a solar-assisted absorption cooling system as a sustainable alternative for Libya's cooling requirements. This study aims to improve solar energy applications in cooling and facilitate Libya's transition to a more sustainable energy future through a comprehensive system performance and operational efficiency analysis.

1.8. OBJECTIVES

This thesis delineates the following aims in response to the pressing demand for sustainable air conditioning solutions in arid locations:

- To evaluate the thermodynamic and exergy performance of a solar-driven absorption cooling system under different climatic conditions in Libya (Tripoli, Benghazi, and Misrata).
- To analyze the impact of operational parameters on system efficiency and optimization of solar cooling performance.
- To explore the feasibility of implementing a solar-assisted absorption cooling system as a sustainable alternative to conventional cooling methods in Libya.

1.9. ORGANIZATION OF THE THESIS

To systematically address the objectives, this thesis is structured as follows:

- *Chapter 1: Introduction*

Provides an overview of human comfort needs, solar energy fundamentals, parabolic trough collectors, solar-powered cooling approaches, and the significance of absorption chiller systems. It also outlines the weather data for three selected Libyan cities and clarifies the primary objectives and the thesis structure.

- *Chapter 2: Literature Review*

Presents a comprehensive survey of existing research on solar cooling technologies, with special attention to parabolic trough applications, absorption chillers, and documented case studies relevant to Libya and similar climates.

- *Chapter 3: Methodology*

Details the methodological framework adopted in this thesis, including the solar-assisted air conditioning system's design, modeling assumptions, parabolic trough collectors' configuration, and absorption chiller parameters. Outlines the parametric study design and the metrics used for performance and economic evaluations.

- Chapter 4: Results and Discussion

Reports on the findings from the simulations and parametric analyses. Examine the influence of city-specific weather conditions on system performance and compare results across the three regions.

- *Chapter 5: Conclusions*

Summarizes the key conclusions drawn from the research.

CHAPTER 2

LITERATURE REVIEW

The rising demand for eco-friendly, energy-efficient cooling has spurred considerable research into solar-powered air conditioning systems, especially in areas with strong solar resources. By using the sun's energy to drive the cooling process, these systems offer a cleaner, more sustainable alternative to traditional air conditioners that depend on fossil fuels—thereby lowering greenhouse gas emissions. This chapter examines key studies on designing, analyzing, and optimizing solar cooling solutions, emphasizing the integration of absorption chillers, the role of solar collectors, and the impact of local climate conditions on system efficiency.

Soussi et al. [38] used TRNSYS software to create a dynamic simulation model that links a solar cooling system with a building. They ran simulations under real-world conditions to gauge performance and spot possible improvements. When they compared their model to data gathered in a summer 2015 field study, they found that the solar collectors achieved efficiencies ranging from 26% to 35%, and the system's coefficient of performance (COP) varied between 0.65 and 1.29. At its peak, the daily COP from the solar input alone reached about 35%. However, the system still failed to meet 32.3% of the cooling demand, meaning the absorption chiller only ran for 53.8% of the total operational time. To address this shortfall, the researchers proposed adding an auxiliary heater before the chiller and increasing the aperture area to raise driving temperatures and optimize chiller performance. After these updates, chiller operation jumped to 75.8%, cooling output rose by 75.6%, and the solar COP climbed to 57%. Meanwhile, the solar fraction averaged 87% over the study period.

Musbah et al. [39] created a mathematical model for a flat-plate solar collector system paired with a single-effect $LiBr/H_2O$ absorption chiller. Their goal was to see if a solar-powered air conditioning setup would be practical for an office building in Libya.

They ran various analyses to determine the total solar radiation that hits a tilted collector surface, finding that the building needed about 884 MWh of heat to meet its cooling requirements during the entire season. Of that amount, roughly 302 MWh could be supplied by the solar collectors, while an auxiliary gas-fired boiler covered the remaining 582 MWh. By installing 1400 m² of collector area, the team achieved a maximum solar fraction of 48%.

Wrobel et al. [40] explored a hybrid cooling system that merges an electric chiller with a desiccant wheel for dehumidification, supported by a chilled ceiling to handle sensible heat loads. They developed a mathematical model—validated with data from an open-cycle desiccant-assisted air conditioning system in Hamburg—to evaluate performance across multiple locations and examine how different operating conditions affect dehumidification needs. According to their findings, the desiccant-assisted AC system significantly decreased both peak and overall energy use compared to a conventional HVAC setup. Specifically, it slashed peak cooling power requirements to between 28% and 32%, while the maximum heat demand dropped to around 30% to 51% of what a standard system would need. These energy gains were closely tied to operating hours and conditions, with less humid regions reaping smaller benefits. However, areas with high humidity, especially when combining desiccant wheels and pre-cooling coils, saw notable improvements in energy efficiency.

Baniyounes et al. [41] explored the development and challenges of solar-assisted air conditioning systems, particularly within Australia's subtropical regions. The study pointed out that, globally, most solar cooling technologies remain at the demonstration phase, with ongoing efforts to improve performance, reduce equipment size, and enhance affordability. While interest in solar cooling has increased in Australia, most projects have been limited to major cities and focused primarily on energy efficiency, often neglecting indoor air quality. Specifically, in Central Queensland, high humidity levels have heightened HVAC demand, leading to greater energy consumption and indoor air quality issues such as mold growth. The study emphasized the importance of designing small-capacity solar cooling systems that maintain air quality in high-occupancy institutional buildings. Furthermore, it highlighted the potential of solar cooling to reduce fuel use and emissions but also acknowledged barriers such as high

upfront costs and limited technical knowledge. To enhance adoption, the authors recommended improving solar collector performance, lowering equipment costs, and promoting a broader understanding of the long-term environmental and energy benefits associated with solar-assisted cooling systems. To fully realize these benefits, the study recommends reducing equipment costs, improving collector efficiency, and fostering a broader understanding among designers and operators of the long-term value of solar cooling in achieving low-emission, energy-independent buildings.

Gude and Nirmalakhandan [42] introduced an innovative desalination method that utilizes low-grade thermal energy, enabling freshwater production through low-temperature distillation under near-vacuum conditions. This setup relies on a thermal energy storage (TES) system maintained at 55 °C, which can be powered by waste heat or renewable sources. Their study specifically evaluated the feasibility of using heat rejected from a modified absorption refrigeration system (ARS) as the energy source for desalination. The ARS, with a cooling capacity of 3.25 kW, provided enough residual heat to distill approximately 4.5 kg of water per hour, requiring only 208 kJ/kg of freshwater produced. This energy demand is lower than traditional methods like multi-stage flash distillation. The system also integrated solar collectors and grid power to supply the ARS generator. Simulation models revealed a desalination efficiency between 80–90%, with a required TES volume of 10 m^3 and solar collector area of 25 m^2. The authors concluded that the system offers a sustainable solution for simultaneous cooling and desalination, particularly when powered entirely by renewable or waste heat sources. Efficiency could be further improved by adopting double or triple-effect configurations, making it a promising approach for regions facing both water scarcity and high cooling demands.

Ma et al. [43] conducted a comprehensive study on the feasibility of solar-assisted cooling technologies for office buildings across various Australian climate zones, analyzing their technical, environmental, and economic viability. Using EnergyPlus simulations, the study assessed three solar cooling systems: the SDEC (solar desiccant evaporative cooling), SDCC (solar-driven conventional cooling), and SAC (solar absorption cooling) systems. Results indicated that solar cooling is technically practical across the country, with the SDEC system consistently delivering the best

performance in terms of solar fraction (SF) and system COP. Notably, in hot and humid areas like Darwin, the SDEC system achieved an annual SF of 0.82 and an electric COP of 25.5, while in cooler regions like Hobart, these values were lower at 0.49 and 1.12 respectively. Across most locations, all three systems used less energy than traditional VAV systems, with the SDEC system offering the highest energy savings and CO_2 reduction—saving up to 82.1% of electricity and cutting 178.45 tonnes of emissions in Darwin. Economically, all systems were viable in Darwin due to favorable payback periods and positive net present values, while the SDEC system remained cost-effective in cities like Brisbane and Sydney. In contrast, colder climates such as Canberra and Hobart saw limited economic benefit due to higher upfront costs and lower energy savings, suggesting that reducing initial costs could improve viability in these regions.

Ibrahim et al. [44] presented an economic assessment of a solar-assisted air conditioning system that integrates a parabolic trough solar collector (PTC), a double-effect water-lithium bromide (H_2O–LiBr) absorption chiller, and a novel absorption energy storage (AES) unit. The system was designed to operate under the climatic conditions of Eastern Saudi Arabia, aiming to extend cooling coverage by utilizing stored thermal energy. The analysis, based on the annuity method, revealed that the system could achieve a payback period of approximately five years for a commercial building. The study found that supplementing a traditional vapor-compression system with this solar-driven setup led to significant energy savings, especially during peak summer months like July and August, where up to 58% reduction in energy use was observed. Moreover, a solar fraction of 63% was achieved, indicating that most of the cooling demand could be met by solar energy. Financially, the system demonstrated an annual levelized energy cost savings of around USD 137,944. Ibrahim emphasized that the system's economic performance improved with higher electricity rates and that integrating AES significantly enhanced energy efficiency and sustainability. The study provides a valuable reference for future designs of energy-efficient cooling systems, particularly in sun-rich regions with high cooling demands.

Vakiloroaya [45] proposed an innovative enhancement to a newly developed direct expansion air conditioning system by integrating it with a vacuum solar collector

positioned downstream of the compressor. This configuration includes a bypass line and a three-way proportional control valve in the compressor's discharge line, enabling precise regulation of refrigerant flow based on real-time temperature readings—specifically, the refrigerant temperatures after the compressor, exiting the solar storage tank, and the ambient dry-bulb temperature. To optimize system performance, a generalized optimization algorithm was developed using sequential quadratic programming (SQR) alongside an empirical model that defines the objective function. The goal was to determine the ideal refrigerant temperature entering the condenser to maximize efficiency. Simulation results from a transient analysis tool provided optimal set-points, which were then used as references in an online closed-loop controller. The system was thoroughly instrumented for data collection, and findings demonstrated that operating at higher subcool temperatures post-condenser led to a substantial improvement in the system's overall coefficient of performance (COP). This approach effectively leverages solar energy to boost cooling efficiency, making it a promising solution for energy-efficient air conditioning.

Akyüz et al. [46] conducted an experimental study to evaluate the potential of solar-assisted air conditioning systems in reducing energy consumption and environmental impact in residential buildings. Recognizing that HVAC systems are among the most energy-intensive elements in buildings, the study investigated the performance of air conditioners equipped with a solar heating mechanism prior to the compressor inlet. Tests were carried out in two identical rooms under outdoor temperatures of 32°C, 36°C, and 38°C, while maintaining indoor temperatures at 18°C, 19°C, and 20°C. The results demonstrated that pre-heating the refrigerant could lead to energy savings between 8% and 28%, depending on the compressor inlet temperature. A life-cycle assessment further showed that this reduction in energy use corresponded to a decrease in emissions ranging from 7.74% to 28.27%. Notably, this approach not only reduced compressor energy consumption but also enhanced the durability of AC systems by preventing wet vapor entry into the compressor. The study emphasized that utilizing solar energy, particularly during peak sunlight hours, aligns perfectly with cooling demand, thereby offering significant potential for sustainable energy savings and emissions reduction. Moreover, implementing solar-powered AC systems at scale could ease urban energy demand and promote economic opportunities in renewable

energy sectors. Akuz suggested that future research should explore the optimal compressor inlet temperatures through both experimental and AI-driven optimization methods to further enhance system efficiency.

Al-Ugla et al. [47] explored the techno-economic feasibility of integrating solar energy into air conditioning systems in Saudi Arabia, where HVAC systems account for approximately 65% of electricity use in buildings. The study compared conventional vapor-compression, solar LiBr–H_2O absorption, and solar PV-powered vapor-compression systems for a large commercial building in Khobar City under consistent daytime cooling demands. Results showed that solar absorption systems were more economically viable than PV-driven systems, particularly as building size and electricity tariffs increased. At higher rates (up to \$0.16/kWh), the payback period (PBP) for the solar absorption system dropped to 9 years compared to 10 years for the PV system, while the net present value (NPV) was also higher (\$2.65 million vs. \$2.15 million). Additionally, solar absorption systems achieved a maximum coefficient of performance (COP) of 1.421 and second law efficiency of 0.538. Government subsidies halved payback periods, further enhancing feasibility. Technically, improving system COP by optimizing condenser and evaporator temperatures had a positive impact on both PBP and NPV. The findings suggest that solar absorption cooling presents a practical solution to reduce peak power demand, enhance energy efficiency, and mitigate environmental impact in energy-intensive regions like Saudi Arabia.

Aguilar-Jiménez et al. [48] examined the implementation of a 35-kW solar-powered absorption cooling system in a remote, off-grid school in Puertecitos, Mexico—an area facing significant resource limitations. Fueled by a 110 m^2 field of evacuated tube solar collectors, the system provided cooling to four classrooms using individual 8.75 kW coils and was supported by thermal energy storage to ensure continuous operation during weekdays. Simulations conducted using TRNSYS software assessed system performance under local conditions, such as water scarcity and limited energy infrastructure. Findings revealed that the system could reliably meet cooling needs for five school days under full load, provided weekends were used for thermal storage recharge. Moreover, operating at 75% load or less allows uninterrupted cooling

throughout the week without additional recharge periods. A critical challenge identified was the system's daily water demand of 750 kg, leading to using a dual water circuit that allows seawater in the cooling tower to mitigate freshwater scarcity. The study demonstrated that solar thermal systems can sustainably deliver comfort in marginalized, isolated communities with strategic energy and water management. It also provided practical system operation, maintenance, and resource optimization guidelines tailored to real-world conditions.

Baniyounes et al. [49] conducted a feasibility study on implementing solar-assisted air conditioning systems in three subtropical regions of Central Queensland, Australia—Rockhampton, Gladstone, and Emerald—where high solar availability coincides with significant cooling demands. The research evaluated energy performance using TRNSYS simulations for reference office buildings. It analyzed primary energy savings when replacing 80% of the energy consumption of a conventional vapor compression system (COP 2.5) with solar energy. Results indicated that 50 m^2 of solar collectors and varying hot water storage volumes could yield substantial savings. For instance, in Emerald, energy savings reached 73% with 0.3 m^3 of storage, increasing to 88% with 1.8 m^3. Similar improvements were observed in Gladstone (69% to 82%) and Rockhampton (62% to 80%). Despite the challenges of high installation costs and limited technical knowledge among stakeholders, the study highlighted that solar cooling systems could significantly reduce energy use and greenhouse gas emissions, offering a sustainable solution for Australia's climate. Integrating these systems with conventional air conditioning enhances indoor air quality while minimizing environmental impact. The findings underscore the importance of further research and development to optimize system design, improve cost-effectiveness, and increase adoption in commercial and residential sectors.

Rosiek et al. [50] evaluated the effectiveness of integrating chilled water storage tanks into a solar-assisted air conditioning system at the Solar Energy Research Center. The system, comprising solar collectors, an absorption chiller, a cooling tower, an auxiliary heater, and both hot and chilled storage tanks, aimed to enhance energy efficiency through optimized operation. By analyzing the building's cooling load dynamics, the study introduced a refined operation sequence leveraging chilled water storage to

reduce energy and water consumption. Results showed a 20% reduction in total energy use and 30% savings in water, along with a 1.7-ton decrease in CO_2 emissions over the summer. The chilled storage tanks helped smooth chiller operation, especially during part-load and morning startup periods, while minimizing deionized water use and outdoor noise levels. The system was optimized by utilizing existing chilled water pumps, avoiding additional energy costs. Despite space limitations for on-site storage, integrating chilled water storage significantly improved system performance and sustainability, showcasing its potential for wider application in solar cooling designs.

Ren et al. [51]conducted a simulation-based study to explore how integrating solar energy, thermal energy storage (TES), and demand-side management (DSM) strategies could enhance the energy flexibility of net-zero energy (NZE) buildings. Using TRNSYS, the study modeled 40 different configurations of a solar-assisted air conditioning system combining photovoltaic/thermal (PV/T) collectors, a phase change material-based TES unit, and four DSM strategies, including pre-heating/cooling and temperature set-point adjustments. The simulations revealed that employing DSM alone could achieve a solar contribution of 0.79, while the addition of TES increased it close to 1.0, nearly eliminating grid dependence. However, this improvement came with increased heat pump energy use, rising from 280 kWh to 1,380 kWh annually, highlighting a trade-off between energy independence and consumption. Appliances remained the primary contributors to peak grid import, even in optimized scenarios. The research demonstrated that while DSM alone enhances flexibility, combining it with PV/T and TES maximizes efficiency. However, strategies like temperature set-point relaxation could compromise thermal comfort. These insights support the advancement of NZE building designs, emphasizing the need for integrated thermal and electrical storage solutions to manage peak loads and enhance sustainability.

Rosiek [52] also analyzed the thermal performance of a solar-assisted air conditioning system equipped with chilled water storage tanks, focusing on improving efficiency under real operating conditions. The system, incorporating flat-plate collectors and an absorption chiller, demonstrated that synchronizing the operation of solar collectors, chiller, and storage tanks could significantly reduce energy losses. The study

emphasized the need for better control strategies to manage the mismatch between energy production and demand, particularly in renewable systems. By optimizing the system's operation—such as operating the absorption chiller at lower inlet temperatures and adjusting the temperature profiles of the storage tanks—the research highlighted potential reductions in auxiliary heating and enhancements in overall energy efficiency. The findings supported the importance of integrated energy management and system design to maximize solar energy use, reduce operational inefficiencies, and improve the long-term viability of solar-assisted cooling systems.

Chen et al. [53] investigated the performance of a solar-assisted hybrid air conditioning system that integrates an air-cooled adiabatic absorption chiller with a vapor compression refrigeration unit. The study compared two operational modes—cascade and subcooling—from thermodynamic and economic perspectives. Experimental and simulation results revealed that the cascade mode significantly boosted the electric COP (63.9%–166.7% increase), while the subcooling mode, though achieving lower COP gains (15.9%–29.8%), excelled in exergetic efficiency, primary energy efficiency, and lower thermal energy consumption. Economically, the subcooling mode driven by compound parabolic collectors (CPC) was more suitable for residential use due to its lower levelized cost of cooling (0.06 USD/kWh), shorter payback time (8.54 years), and smaller collector area requirement (11.41 m^2). In contrast, while the cascade mode provided higher COP, it required a larger collector area and had higher heat consumption, making it less viable for compact residential installations. Chen's findings offer practical guidance for designing cost-effective and efficient solar-assisted hybrid cooling systems tailored to specific application needs.

Vakiloroaya et al. [54] conducted an experimental study on a hybrid solar-assisted direct expansion air conditioning system paired with a vacuum solar collector to address the growing need for energy-efficient and environmentally friendly cooling solutions. Mathematical models of the system components were developed and validated against empirical data, and extensive instrumentation was used to monitor system performance. The study focused on how factors such as average water temperature, storage tank size, and indoor temperature settings influenced energy use. A key finding was that once the desired room temperature was reached, the compressor

could remain off for extended periods, with cooling continuing through heat transfer from the storage tank to the refrigerant. This feature significantly improved energy efficiency, resulting in monthly savings ranging from 25% to 42%. The system's design effectively reduced compressor operation time, thereby lowering electricity consumption and operational costs, and demonstrated a promising approach to sustainable air conditioning using renewable solar energy.

Habib et al. [55] conducted seasonal transient simulations using TRNSYS to evaluate an Integrated Absorption Desiccant System (IADS) designed to handle sensible and latent cooling loads separately, with peaks of 10.94 kW and 4.44 kW, respectively. Radiant cooling supplied by an absorption chiller managed the sensible load, while a solid desiccant dehumidification system addressed the latent component. Key system elements, including flat plate solar collectors, desiccant wheel, heat recovery wheel, and absorption chiller, were modeled and coupled with GenOpt for optimization. Results revealed that the standalone absorption system achieved a solar fraction of 57.5% and a thermal COP of 0.55, while the IADS reached 56.2% solar fraction and a higher COP of 1.52. The study also examined how varying the ratio of sensible to latent loads impacted regeneration heat requirements, identifying a critical load ratio of 0.75. These insights offer valuable guidance for HVAC designers to optimize system efficiency and energy use, especially during early-stage design processes by separating load management strategies.

Rahman et al. [56] designed and simulated an absorption-based solar air conditioning system aimed at domestic applications using the TRNSYS platform, tailored to the climate conditions of Lahore, Pakistan. The system featured. five interconnected thermal loops, including evacuated glass tube solar collectors with R-410A refrigerant, a hot water tank with a heat exchanger, an absorption chiller, an auxiliary furnace, a cooling tower, a chilled water loop, and an air distribution network. Parametric studies identified optimal performance settings, achieving a collector outlet temperature averaging 78°C, with a peak temperature of 199°C, and a heat gain of 71,065 kJ/h. The storage tank maintained an average of 92°C, delivering cooling at varying room temperatures (27°C, 30°C, 19°C). The furnace operated at 41.67 kW capacity, and the system's cooling coils had a sensible cooling capacity of 22 kW. Notably, the system

ran entirely on solar thermal energy without auxiliary electricity, demonstrating its potential for sustainable cooling. These results highlight the feasibility of using low-grade solar thermal energy to meet domestic cooling demands while maintaining indoor comfort. This makes it a viable solution for energy-efficient and environmentally friendly air conditioning.

Chen et al. [57] experimentally evaluated a solar-assisted hybrid absorption-compression system designed to provide year-round heating and cooling while maximizing solar thermal energy utilization. The system combined an absorption heat pump and vapor compression subsystem, enabling efficient operation at lower driving temperatures (as low as 60°C), thereby improving solar collector efficiency. Comparative performance analysis with traditional air-source heat pumps demonstrated that, under solar-assisted heating conditions with hot water at 80°C, the system achieved a 45.8% increase in electric COP (COPele) and a 31.4% power-saving ratio (PSR). The improvements were 18.9% and 16.0% in cooling mode, respectively. The study also found that compressor speed significantly influenced heating performance more than cooling, and higher fan frequency improved heating effectiveness. Moreover, the energy-saving ratio (ESR) ranged from 19.8% to 23.9% in heating and from 19.9% to 25.1% in cooling. Despite promising results, Zhao emphasized the need for further optimization in subsystem design, refrigerant charge testing, and control strategy to ensure efficiency under variable operating conditions. This research demonstrates the potential of hybrid systems in reducing energy consumption and supporting decarbonization in the building sector.

Hidalgo et al. [58] carried out an experimental study on solar absorption cooling at Universidad Carlos III de Madrid (UC3M) to explore environmentally friendly alternatives to conventional air conditioning in Spain, where summer temperatures often exceed 35°C. The system utilized 50 m² of flat-plate solar collectors to power a single-effect $LiBr/H_2O$ absorption chiller through a hot water storage tank. Data collected at 10-minute intervals during the summer of 2004 indicated that the chiller delivered a cooling power of 6–10 kW with an input of 10–15 kW, maintaining full solar autonomy for an average of 6.5 hours per day. The system's output was compared to the cooling needs of a 90 m² detached house to assess practical applicability,

revealing that the setup could cover 56% of the seasonal air conditioning load. A sensitivity analysis on solar field sizing confirmed that the system was properly dimensioned. Moreover, the study highlighted notable reductions in electricity use, refrigerant leakage, and environmental impact compared to conventional vapor-compression units, making it a viable and sustainable alternative for residential cooling in sunny climates.

While numerous studies have explored the performance of solar-assisted air conditioning systems globally, there is a noticeable lack of research specifically addressing the application and optimization of such systems in Libya's diverse climatic regions. Existing work has primarily focused on generalized models or individual case studies, often neglecting the influence of local environmental parameters such as solar irradiance variability, ambient temperature ranges, and humidity levels specific to Libyan cities like Tripoli, Benghazi, and Misrata. Moreover, many studies fail to integrate detailed energy and exergy analyses under real climatic conditions or explore parametric sensitivity to optimize system performance. This thesis fills this critical gap by conducting a comprehensive thermodynamic and exergy evaluation of a solar-assisted absorption cooling system tailored to Libya's major climate zones, aiming to determine optimal operational settings and assess feasibility for large-scale deployment. By doing so, the study contributes valuable insights toward sustainable cooling solutions in arid and semi-arid regions with high solar potential.

CHAPTER 3

SYSTEM MODELING AND METHODOLOGY

This chapter presents the methodological framework employed to analyze the performance of a solar-assisted absorption air conditioning system designed for Libyan climatic conditions. The study integrates both energy and exergy analyses to assess the efficiency and sustainability of the system under varying environmental and operational parameters. The model incorporates Parabolic Trough Collectors (PTC) as the primary solar energy input, coupled with a LiBr–H_2O absorption cooling cycle. Detailed descriptions of system components, thermodynamic processes, and governing equations are provided to enable simulation and optimization. The methodology also outlines the assumptions, parameters, and equations used to calculate thermal and exergetic performance indicators, which serve as the basis for the results and discussion in the following chapters.

3.1. SYSTEM DESCRIPTION

Figure 1 presents the concentrated solar energy (PTC - Parabolic Trough Collectors), which operates an absorption cooling cycle based on lithium bromide and water (LiBr-H_2O). The system uses solar energy as a heat source to operate a thermal generator that separates water from the lithium bromide solution, allowing for an efficient and environmentally friendly cooling cycle. The main components of the system include:

- **Solar PTC Field:** This field captures and concentrates sunlight to heat a heat transfer fluid (such as water or thermal oil).
- **Thermal Storage Tank**: Store excess heat energy for use during low solar radiation or at night.

- **Circulating Pumps (P1, P2, and P3):** P1 and P2 are used to transfer the heated fluid between the solar collectors and the thermal tank, and P3 Pumps the LiBr-H_2O solution into the system.
- **Generator:** The LiBr-H_2O solution is heated using the heat from the solar collectors. The water evaporates and separates from the solution, heading to the condenser, while the concentrated lithium bromide returns to the heat exchangers.
- **Heat exchanger (SHEX - Solution Heat Exchanger):** Used to exchange heat between the concentrated solution and the one returning to the absorber, increasing the efficiency of the thermal system.
- **Condenser:** Condenses the separated water vapor in the heat generator and converts it to liquid water under low pressure.
- **First expansion valve (EV_1):** Reduces the pressure and cools the liquid water heading to the evaporator.
- **Evaporator:** Absorbs heat from the surrounding atmosphere or inside the building, cooling the desired space.
- **Absorber:** Absorbs the water vapor resulting from the evaporator and remixes it with the lithium bromide to restart the cycle.
- **Second Expansion Valve (EV_2):** Helps regulate the flow of LiBr-H_2O solution within the system.
- **Cooling Building:** Cool air is sent into the building to provide the required cooling.

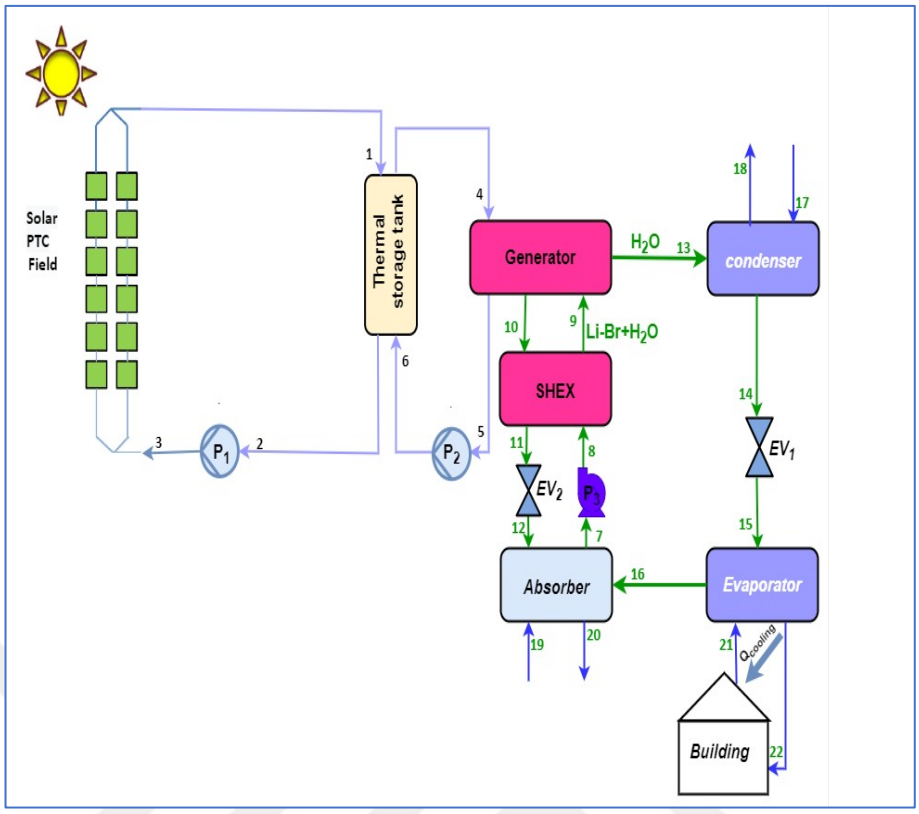

Figure 3.1. Schematic diagram of a solar absorption cooling system for libyan cities (Tripoli, Benghazi, and Misrata)

3.1.1. Assumptions and Inlet Parameters

Table 3.1 presents the input data for modeling the proposed solar absorption cooling system. The system modeling is carried out based on the following assumptions:

- Each component of the system is assumed to operate under steady-state conditions.
- Pressure drops in piping and the heat exchanger are negligible due to their minimal effect, except for the notable pressure drops across the expansion valves between points 11 and 12 and 14 and 15 (refer to Fig. 3.1).
- The working fluid is assumed to exit the condenser as a saturated liquid and the evaporator as a saturated vapor.
- The work input by the circulating pump is disregarded, as it is insignificant compared to the thermal energy supplied to the generator.

- Exergy calculations are based on the specific enthalpy and entropy values of water at standard environmental conditions (25 °C and 1 atm).
- Kinetic and potential energy and exergy contributions are ignored due to their relatively minor influence on the system.

Table 3.1. Input data for modeling of the suggested system.

Parameter	Value
Solar area (m^2)	71.16 m^2
Sun temperature	5770 K
DNI	7.92 kWh/ m^2.day
PTC outlet temperature	243° C
PTC inlet temperature	120.1° C
T_{amb}	25° C
P_{amb}	101kPa
Absorber temperature (T_7)	33° C
Generator temperature (T_{10})	81.39° C
LiBr solution strength	54.3%
Pumps efficiency	80%
Solution heat exchanger effectiveness	57%

3.1.2. System Mechanism

The operation of an absorption cooling system with the help of solar energy is as follows:

- The thermal fluid is heated in the solar collector field and then sent to the thermal tank, which helps regulate the thermal energy supply.
- The heat is transferred from the tank to the thermal generator, where the solution of lithium bromide and water is heated.
- Due to heating, the water evaporates and separates from the LiBr solution, then moves to the condenser, where it is converted into a liquid.
- The liquid water is passed through the first expansion valve (EV_1), which reduces the pressure and temperature, then reaches the evaporator.

- In the evaporator, the liquid water absorbs heat from the building (cooling process) and turns into steam.
- The water vapor is transferred to the absorber and absorbed by the LiBr-H_2O solution, which reconstitutes the initial solution.
- The solution is pumped back from the absorber to the generator via the pump (P_3) to repeat the cycle.

3.1.3. Benefits and Applications in Libyan Cities

A solar-assisted absorption cooling system's effectiveness is closely linked to its operating environment's climatic conditions. This section examines how the system was adapted and utilized in three major Libyan cities (Tripoli, Benghazi, and Misrata), each with its own thermal characteristics and solar radiation levels. The goal is to demonstrate the feasibility and energy-saving potential of the system in different regional contexts.

- **Tripoli:** It is characterized by high temperatures and medium humidity, which makes this system an ideal solution to improve cooling efficiency with minimal energy consumption.
- **Benghazi:** Moderate to hot climate, but relying on this system will help reduce pressure on the electrical grid, especially in the summer.
- **Misurata:** The city is exposed to high heat waves at some times, and therefore the system can provide a comfortable indoor environment for residential and commercial buildings.

3.1.4. System Features

The key features that make the proposed solar-assisted absorption cooling system an effective and sustainable solution under the prevailing climatic conditions in Libyan cities can be summarized as follows:

- Clean and sustainable energy - relies on solar energy to reduce fossil fuel consumption.

- High efficiency - combines cooling and heating using recovered heat.
- Low operating costs - does not require large electricity as in traditional cooling systems.
- Suitable for the Libyan climate - can operate effectively in the hot and dry conditions Libyan cities face.

3.2. ENERGY ANALYSIS OF THE INTEGRATION SYSTEM

The fundamental concepts of continuity and the first law of thermodynamics are summarized below [59,60]:

$$\sum_{in} \dot{m}_{in} = \sum_{out} \dot{m}_{out} \tag{3.1}$$

$$\sum_{in} \dot{m}_{in}\, \mathrm{x}_{in} = \sum_{out} \dot{m}_{out}\, x_{out} \tag{3.2}$$

where $\dot{m}_{in}$ is the entered mass flow rate, $\dot{m}_{out}$ is the exit mass flow rate, x_{in} is the LiBr concentration at the inlet and x_{out} is the LiBr concentration at the outlet.

The following equation allows us to model energy interactions in steady-state processes. It ensures a comprehensive energy analysis and highlights efficiency and losses in the system [61,62]:

$$\dot{Q}_{in} + \dot{W}_{in} + \sum_{in} \dot{m}(h_{in}) = \dot{Q}_{out} + \dot{W}_{out} + \sum_{out} \dot{m}(h_{out}) \tag{3.3}$$

Where: "$\dot{W}$" refers to the work produced, "$\dot{m}$" refers to the mass flow rate,"$\dot{Q}$" refers to the heat input, and "h" refers to the enthalpy. The letters 'in' and 'out' in the subscript denote the inlet and output states.

The energy balance equations for the integration system components are shown below.

- *Solar Energy Collection:*

Thermal energy received by the collector is calculated as follows [63]:

$$\dot{Q}_{solar} = \eta_{PTC} * A_a * DNI \tag{3.4}$$

Where, "$\dot{Q}_{solar}$", represents to the thermal energy for PTC,"A_a", refers to the solar areas, "DNI", refers to the direct normal irradiance, and"η_{PTC}", demonstrates the PTC's efficiency.

The following equations are used to calculate the available solar energy for the system [63,64]:

$$\dot{Q}_u = \dot{m} c_p (T_{out} - T_{in}) \tag{3.5}$$

Where, "$\dot{Q}_u$ "refers to the useful heat gain (kW or kJ/s)," $\dot{m}$" demonstrates the mass flow rate of the working fluid (kg/s),"c_p" refers to specific heat capacity, and" T_{out} and T_{in}" illustrate the temperature difference.

The efficiency of the solar collector η_{PTC} is calculated as the ratio of the useful heat gain $\dot{Q}_u$ to the total solar energy incident on the collector $\dot{Q}_{solar}$ [63,64].

$$\eta_{PTC} = \frac{\dot{Q}_u}{\dot{Q}_{solar}} \tag{3.6}$$

- *Pump1*

The work required to run the pump1 can be calculated from the following equation:

$$\dot{W}_{P_1} = \dot{m}_2 (h_3 - h_2) \tag{3.7}$$

Where "$\dot{W}_{P_1}$" represents the work required by pump1.

- *Thermal Energy Storage (TES):*

The heat loss from thermal energy storage can be determined from the following equation[65]:

$$\dot{Q}_{TES} = (\dot{m}_1 h_1 - \dot{m}_2 h_2) = (\dot{m}_4 h_4 - \dot{m}_6 h_6) \quad (3.8)$$

Where "$\dot{Q}_{TES}$" represents the change in thermal energy stored within the tank.

- *Pump₂*

The work required to run the pump$_2$ can be calculated from the following equation:

$$\dot{W}_{P_2} = \dot{m}_5 (h_6 - h_5) \quad (3.9)$$

Where "$\dot{W}_{P_1}$" represents the work required by pump$_1$.

- *Generator:*

The heat transferred from the generator in the system can be calculated from the following equation:

$$\dot{Q}_G = \dot{m}_4 (h_4 - h_5) = \dot{m}_9 h_9 - \dot{m}_{10} h_{10} + \dot{m}_{13} h_{13} \quad (3.10)$$

Where: "$\dot{Q}_G$" refers to the heat transfer rate through the generator, and" $\dot{m}_9$" represents the mass flow rate of the LiBr-H_2O mixture.

- *Condenser:*

The heat transfer within the condenser in the ARS system can be calculated from the following equation:

$$\dot{Q}_{\text{Con}} = \dot{m}_{13}(h_{13} - h_{14}) \tag{3.11}$$

Where, "$\dot{Q}_{\text{Con}}$" refers to the heat transfer rate through the condenser.

- *Expansion Valves:*

The energy balance for the expansion valves in the ARS system can be calculated from the following equations:

$$\dot{m}_{14}h_{14} = \dot{m}_{15}h_{15} \tag{3.12}$$

$$\dot{m}_{11}h_{11} = \dot{m}_{12}h_{12} \tag{3.13}$$

- *Sensible Heat Exchanger (SHEX):*

The heat transferred within the heat exchanger in the ARS system can be calculated from the following equation:

$$\dot{Q}_{SHEX} = \dot{m}_{10}(h_{10} - h_{11}) = \dot{m}_{9}(h_{10} - h_{9}) \tag{3.14}$$

Where "$\dot{Q}_{SHEX}$" refers to the heat transfer rate through the solution heat exchanger.

- *Evaporator:*

The heat transferred from the evaporator in the system can be calculated from the following equation:

$$\dot{Q}_{\text{Evap}} = \dot{m}_{15}(h_{15} - h_{10}) \ = \dot{m}_{21}(h_{21} - h_{22}) \tag{3.15}$$

Where "$\dot{Q}_{\text{Evap}}$" refers to the heat transfer rate through the evaporator$_2$.

- *Absorber*

The heat absorbed from the absorber in the system can be calculated from the following equation:

$$\dot{Q}_{Abs} = \dot{m}_7 h_7 - \dot{m}_{16} h_{16} - \dot{m}_{12} h_{12} \quad (3.16)$$

Where"$\dot{Q}_{Abs}$" represents the exergy rate for the absorber.

- *Pump₃*

The work required to run the pump₃ can be calculated from the following equation:

$$\dot{W}_{P_3} = \dot{m}_7 (h_8 - h_{17}) \quad (3.17)$$

Where "$\dot{W}_{P_3}$" represents the work required by pump₃.

3.3. EXERGY ANALYSIS OF THE INTEGRATION SYSTEM

The exergy rate is the most useful theoretical work achieved when a system transforms from its initial state to thermal and mechanical equilibrium with its surroundings. The following formula for exergy balance will be used to determine each part's exergy destruction [66,67]:

$$\dot{E}_Q - \dot{E}_W = \sum \dot{E}_{out} - \sum \dot{E}_{in} - \dot{E}_{Dest} \quad (3.18)$$

Where: " $\dot{E}_Q$" refers to the exergy rate for heat transfer (MW)," $\dot{E}_W$" represents the exergy rate for work transfer (MW)," $\dot{E}_{out}$" indicates the exergy rate for system outputs (MW), " $\dot{E}_{in}$" refers to the exergy rate for system inputs (MW), and" $\dot{E}_{Dest}$" refers to the exergy destruction rate (MW).

The stream exergy rate by heat is determined using the following equation [68].

$$\dot{E}_Q = \left(1 - \frac{T_{\text{amb}}}{T_i}\right)\dot{Q}_i \tag{3.19}$$

Where: "T_{amb}", indicates the environment temperature for a dead state (K),"T_i" refers to the system boundary temperature for heat transfer happens (K), and"$\dot{Q}_i$", represents the heat transfer rate (MW).

The exergy balance for a system in a steady state is stated as follows [69]:

$$\dot{E}_f = \dot{E}_p + \dot{E}_{dest} \tag{3.20}$$

Here, $\dot{E}f$, $\dot{E}p$, and $\dot{E}_{dest}$ represent the exergy flow of fuel, product, and destruction, respectively. According to the second law analysis, the exergy destruction rate represents the loss of the ability to convert energy into usable work. To examine a system's exergy efficiency, the fuel and product exergy of each component are evaluated using the surplus efficiency principles [70]:

$$\eta_{\text{ex}} = \left(1 - \frac{\dot{E}_{dest}}{\dot{\text{E}}\text{f}}\right) = \frac{\dot{\text{E}}\text{p}}{\dot{\text{E}}\text{f}} \tag{3.21}$$

where η_{ex}represents the exergy efficiency

- *PTC:*

The exergy of the solar field, associated with solar radiation (Ės), is defined as follows:

$$\dot{E}_{D,PTC} = \left(1 - \frac{T_{amb}}{T_{sun}}\right)\dot{Q}_{solar} - \left(\dot{E}_1 - \dot{E}_3\right) \tag{3.22}$$

Where: "$\dot{E}_{D,PTC}$" refers to the exergy destruction in the PTC (MW),"T_{sun}", represents the effective temperature of the sun (K), and"$\dot{Q}_{solar}$", indicates the solar heat rate energy collected (MW).

- *Pump$_1$*:

The exergy destruction for pump$_1$ can be defined as follows:

$$\dot{E}_{\mathrm{D},P_1} = \left(\dot{E}_2 - \dot{E}_3\right) + \dot{W}_{P_1} \tag{3.23}$$

Where "$\dot{E}_{\mathrm{D},P_2}$ ", represents the exergy destruction rate within pump$_2$.

- *Thermal Energy Storage (TES)*

The following equations quantify the irreversibility or loss of useful energy within the thermal energy storage system

$$\dot{E}_{D,TES} = \left(\dot{E}_1 - \dot{E}_2\right) - \left(\dot{E}_4 - \dot{E}_6\right) \tag{3.24}$$

Where "$\dot{E}_{\mathrm{D,TES}}$", denotes the exergy destruction in the thermal storage tank.

- *Pump$_2$*:

The exergy destruction for the pump$_3$ can be defined as follows:

$$\dot{E}_{\mathrm{D},\,P_2} = \left(\dot{E}_5 - \dot{E}_6\right) + \dot{W}_{P_2} \tag{3.25}$$

Where "$\dot{E}_{\mathrm{D},\,P_2}$ ", represents the exergy destruction rate within pump$_2$.

- *Generator*:

The exergy destruction for the generator can be defined as follows:

$$\dot{E}_{\mathrm{D},\,\mathrm{G}} = \left(\dot{E}_4 + \dot{E}_5\right) - \left(\dot{E}_{10} + \dot{E}_{13} - \dot{E}_7\right) \tag{3.26}$$

Where "$\dot{E}_{\mathrm{D,\,G}}$ ", refers to the generator's exergy destruction rate.

- *Expansion Valves:*

$$\dot{E}_{\mathrm{D},\,EV_1} = \dot{E}_{14} - \dot{E}_{15} \tag{3.27}$$

$$\dot{E}_{\mathrm{D},\,EV_2} = \dot{E}_{11} - \dot{E}_{12} \tag{3.28}$$

Where, "$\dot{E}_{\mathrm{D},\,EV_1}$, and $\dot{E}_{\mathrm{D},\,EV_2}$ " refers to the exergy destruction rate of the Expansion Valves 1 and 2.

- *Condenser:*

The exergy destruction for the condenser$_3$ can be defined as follows:

$$\dot{E}_{\mathrm{D,\,Con}} = \left(\dot{E}_{13} - \dot{E}_{14}\right) - \left(\dot{E}_{18} - \dot{E}_{17}\right) \tag{3.29}$$

Where "$\dot{E}_{\mathrm{D,\,Con}}$ ", refers to the exergy destruction rate of the condenser.

- *Evaporator:*

The exergy destruction for the evaporator$_2$ can be defined as follows:

$$\dot{E}_{\mathrm{D,\,Evap}} = \left(\dot{E}_{21} + \dot{E}_{22}\right) - \left(\dot{E}_{16} - \dot{E}_{15}\right) \tag{3.30}$$

Where "$\dot{E}_{\mathrm{D,\,Evap}}$ " indicates the exergy destruction rate of the evaporator$_2$.

- *Absorber*

The following equations quantify the irreversibility or loss of useful energy within the absorber:

$$\dot{E}_{\mathrm{D,Abs}} = \left(\dot{E}_7 - \dot{E}_{16} - \dot{E}_{12}\right) - \left(\dot{E}_{20} - \dot{E}_{19}\right) \quad (3.31)$$

Where "$\dot{E}_{\mathrm{D,\,Abs}}$", represents the exergy destruction rate within the absorber.

- *Heat Exchanger*

The exergy destruction for the heat exchanger can be defined as follows:

$$\dot{E}_{\mathrm{D,\,SHEX}} = \left(\dot{E}_{10} + \dot{E}_{11}\right) - \left(\dot{E}_9 - \dot{E}_8\right) \quad (3.32)$$

Where "$\dot{E}_{\mathrm{D,\,SHEX}}$ ", represents the exergy destruction rate within the sensible heat exchanger.

- *Pump₃*:

Exergy destruction for the pump$_3$ can be defined as follows:

$$\dot{E}_{\mathrm{D},P_3} = \left(\dot{E}_7 - \dot{E}_8\right) + \dot{W}_{P_3} \quad (3.33)$$

Where "$\dot{E}_{\mathrm{D},P_3}$ ", represents the exergy destruction rate within pump$_3$.

3.4. TOTAL SYSTEM PERFORMANCE

The coefficient performance of the absorption system (COP) is given as:

$$COP = \frac{\dot{Q}_{\mathrm{Evap}}}{\dot{Q}_{\mathrm{Gen}}} \quad (3.34)$$

The energetic efficiency of the system is assessed using the system coefficient of performance (SCOP), which is defined as follows:

$$SCOP = \frac{\dot{Q}_{\mathrm{Evap}}}{\dot{Q}_{\mathrm{Solar}}} \quad (3.35)$$

The system exergy efficiency (ηex) is defined as:

$$\eta_{ex} = \frac{\dot{Q}_{\text{Evap}} \cdot \left(\frac{T_0}{T_e} - 1\right)}{\dot{Q}_{\text{Solar}} \cdot \left[1 - \frac{4}{3} \cdot \frac{T_0}{T_{\text{sun}}} + \frac{1}{3} \cdot \left(\frac{T_0}{T_{\text{sun}}}\right)^4\right]} \tag{3.36}$$

Table 3.2 summarizes the energy and exergy balance equations for each component of the Model 3 system.

Table 3.2. Energy and exergy balance equations for all components of the Model 3 system.

Component	Energy Balances	Exergy Balances
PTC	$\dot{Q}_{solar} = \eta_{PTC} * A_{ap} * DNI$	$\dot{E}_{Q,solar} = \left(1 - \frac{T_0}{T_{sun}}\right) \dot{Q}_{solar}$
TST	$\dot{Q}_{TST} = \dot{m}_{17}(h_{17} + h_{18})$	$\dot{E}_{\text{D,TST}} = \dot{E}_{17} + \dot{E}_{21} - \dot{E}_{19} - \dot{E}_{18}$
Pump1	$\dot{W}_{\text{P1}} = \dot{m}_9(h_{10} - h_9)$	$\dot{E}_{D,P_1} = \dot{W}_{P1} + \dot{E}_9 - \dot{E}_{10}$
Pump2	$\dot{W}_{\text{P2}} = \dot{m}_{11}(h_{12} - h_{11})$	$\dot{E}_{D,P2} = \dot{W}_{P2} + \dot{E}_{11} - \dot{E}_{12}$
Gen	$\dot{Q}_{Gen} = \dot{m}_{28}(h_{28} - h_{37})$	$\dot{E}_{\text{D,Gen}} = \dot{E}_{28} + \dot{E}_{3*} - \dot{E}_{37} - \dot{E}_{7*} - \dot{E}_{4*}$
Abs	$\dot{Q}_{ARS} = \dot{m}_{1*}h_{1*} - \dot{m}_{6*}h_{6*} - \dot{m}_{10*}h_{10*}$	$\dot{E}_{\text{D,ARS}} = \dot{E}_{10*} + \dot{E}_{6*} - \dot{E}_{12*} + \dot{E}_{13*} - \dot{E}_{1*}$
HEX	$\dot{Q}_{HEX} = \dot{m}_{2*}(h_{3*} - h_{2*})$	$\dot{E}_{\text{D,HEX}} = \dot{E}_{4*} + \dot{E}_{2*} - \dot{E}_{5*} - \dot{E}_{3*}$
Pump5	$\dot{W}_{\text{Pump5}} = \dot{m}_{1*}(h_{2*} - h_{1*})$	$\dot{E}_{\text{D,Pump5}} = \dot{W}_{Pump5} + \dot{E}_{2*} - \dot{E}_{1*}$
Evap2	$\dot{Q}_{Evap\ 2} = \dot{m}_{10*}(h_{10*} - h_{9*})$	$\dot{E}_{\text{D,Evap 2}} = \dot{E}_{10*} + \dot{E}_{22} - \dot{E}_{9*} - \dot{E}_{11*}$
Exv_1	$\dot{m}_{5*}h_{5*} = \dot{m}_{6*}h_{6*}$	$\dot{E}_{\text{D,Ev1}} = \dot{E}_{5*} - \dot{E}_{6*}$
Exv_2	$\dot{m}_{8*}h_{8*} = \dot{m}_{9*}h_{9*}$	$\dot{E}_{\text{D,v2}} = \dot{E}_{2*} - \dot{E}_{9*}$
Cond_3	$\dot{Q}_{Cond_3} = \dot{m}_{7*}(h_{8*} - h_{7*})$	$\dot{E}_{\text{D,Cond 3}} = \dot{E}_{7*} - \dot{E}_{14*} + \dot{E}_{15*} - \dot{E}_{8*}$

CHAPTER 4

RESULTS ANALYSIS

This chapter comprehensively analyzes the simulation results obtained from the thermodynamic and exergy evaluation of the proposed solar-assisted absorption cooling system under varying climatic conditions in Libya's key cities: Tripoli, Benghazi, and Misrata. The chapter systematically investigates how changes in operational parameters, including generator and evaporator temperatures, collector area, solution heat exchanger effectiveness, and direct normal irradiance (DNI), affect system performance in terms of coefficient of performance (COP), exergy efficiency, cooling capacity, and heat transfer behavior across core components.

Table 4.1 presents the thermodynamic state points of the solar-assisted absorption cooling system, detailing key parameters such as mass flow rate, temperature, enthalpy, entropy, and exergy at various locations within the system

Table 4.1. The properties of each state of the solar-assisted absorption cooling system.

State	m	Temperature	Enthalpy	Entropy	x
	(kg/s)	(°CC)	(kJ/kg)	(kJ/kg. K)	(%)
1	0.05703	243	476	1.229	
2	0.05703	120	214.3	0.6525	
3	0.05703	120.1	214.5	0.653	
4	0.05703	223	429.7	1.137	
5	0.05703	113.1	201.3	0.619	
6	0.05703	113.2	201.5	0.6195	
7	0.04706	33.14	78.11	0.2048	0.543
8	0.04706	33.15	78.13	0.2048	0.543
9	0.04706	63.38	140.6	0.3994	0.543
10	0.0428	81.39	195.8	0.4626	0.597
11	0.0428	53.89	142.6	0.3062	0.597
12	0.0428	43.86	142.6	0.3063	0.597
13	0.004257	81.39	2645	7.592	
14	0.004257	38.4	160.8	0.551	
15	0.004257	5	160.8	0.579	
16	0.004257	5	2510	9.025	
17	0.253	25	104.8	0.3672	
18	0.253	35	146.6	0.5051	
19	0.6272	25	104.8	0.3672	
20	0.6272	30	125.7	0.4368	
21	0.1834	18	75.54	0.2678	0.543
22	0.1834	5	21.02	0.07625	

4.1. MODEL VALIDATION

Figure 4.1 presents a validation of the current study's simulation results for the coefficient of performance (COP) and cooling capacity ($\dot{Q}_{Evap}$) against those reported by Balghouthi et al. [71] across a range of generator inlet temperatures (T_4) from 80°C to 120°C. This figure demonstrates successful validation of the current model, as simulation outputs align closely with established data. The current study and the work

by Balghouthi et al., as illustrated in the figure, demonstrate that the COP remains relatively stable with increasing T_4. The current study shows COP values ranging from 0.77 to 0.80, with a slight decline as T_4 increases, suggesting that the system maintains efficiency with minor degradation at higher temperatures. In Balghouthi et al.'s data, COP values are consistently slightly lower (0.76–0.79), but the trend mirrors that of the current study, reinforcing the accuracy and validity of the developed simulation model. The cooling capacity increases noticeably with generator inlet temperature in both studies. In the current study, $\dot{Q}_{Evap}$ rises from 9.9 kW at 80°C to 16 kW at 120°C, demonstrating a strong positive correlation between generator temperature and cooling output. Balghouthi et al.'s results also show an increase from 9 kW to 15.2 kW, slightly below the current study's values across all points.

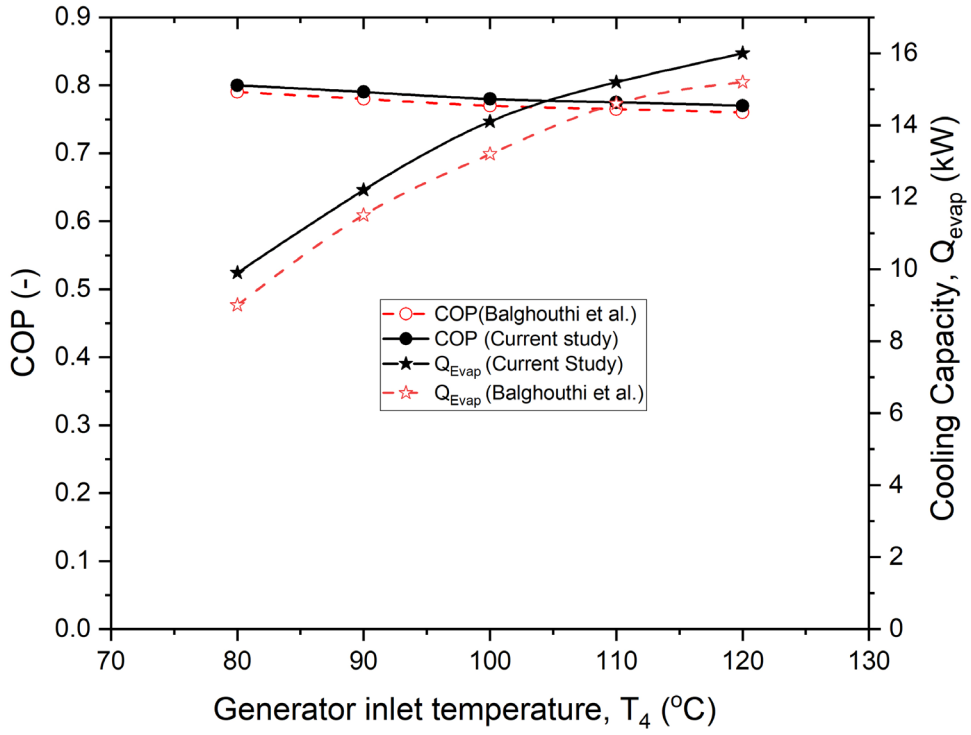

Figure 4.1. Validation of simulation results against literature data for cop and cooling capacity ($\dot{Q}_{Evap}$).

4.2. EXERGY ANALYSIS

Table 4.2 presents a detailed exergy analysis for each major solar-assisted absorption cooling system component. The table includes three key performance metrics: exergy

destruction (kW), percentage of total exergy destruction (%), and exergy efficiency (%). The table highlights that the parabolic trough collector (PTC) is the main source of exergy destruction, drastically affecting overall system efficiency. On the other hand, components like EV_2, TST, Generator, and SHEX demonstrate high exergy efficiency, indicating strong performance in their respective roles. The PTC is the dominant source of irreversibility, accounting for nearly 80% of total exergy destruction, primarily due to large temperature gradients between the solar source and the working fluid. TST has relatively low exergy destruction and high efficiency, suggesting good insulation and thermal management in the storage system. The generator shows high exergy efficiency, indicating that it performs well in utilizing the input thermal energy from the collector. Its moderate exergy destruction reflects conversion losses but remains one of the better-performing units. The condenser suffers from significant irreversibility and low exergy efficiency, likely due to heat rejection to the environment. Enhancing heat recovery or lowering temperature differentials could improve its performance. The absorber shows moderate inefficiency, likely due to mass and heat transfer limitations between the refrigerant and absorbent. There's room for improving absorber design or heat exchanger surface area. The SHEX performs well, contributing minimally to exergy loss while improving internal heat recovery and overall system thermal economy. With moderate exergy destruction and reasonable efficiency, the evaporator plays a stable role in the cooling cycle, though improvements in temperature match between working fluid and surroundings may help.

Table 4.2. Exergy analysis for each solar-assisted absorption cooling system component.

Component	Exergy destruction (kW)	Exergy destruction Percentage (%)	Exergy efficiency (%)
PTC	17.09	79.225	23.41
TST	0.924	4.3	82.33
$Pump_1$	0.0081	0.037	25.81
$Pump_2$	0.0082	0.038	23.39
$Pump_3$	0.0009	0.004	2.425
Generator	1.116	5.2	74.08
Condenser	1.465	6.8	10.91
EV_1	0.035	0.162	84.96
Absorber	0.605	2.8	16.1
EV_2	0.0013	0.006	99.91
SHEX	0.075	0.348	73.72
Evaporator	0.243	1.126	65.96

4.3. PARAMETER ANALYSIS

Figure 4.2 illustrates the impact of generator inlet temperature (T_4) on the coefficient of performance (COP), exergy efficiency, and cooling load in a solar absorption cooling system. As T_4 increases from 170°C to 220°C, the cooling load exhibits a significant upward trend, rising from approximately 5 kW to over 10 kW, indicating that higher generator temperatures enhance the system's cooling capacity. In contrast, the COP remains nearly constant (~0.75–0.8), suggesting the system maintains efficient heat-to-cooling conversion across the temperature range. Similarly, exergy efficiency remains stable at around 0.35, implying that the exergy destruction rate is relatively unaffected by variations in T_4, even though the cooling load increases. The results indicate that increasing the generator inlet temperature does not degrade system efficiency but rather enhances cooling output, making it particularly beneficial for high-demand cooling applications in hot climates such as Tripoli, Benghazi, and Misrata. However, practical constraints such as material limitations, increased energy

consumption, and potential operational costs must be considered when selecting the optimal T_4 value.

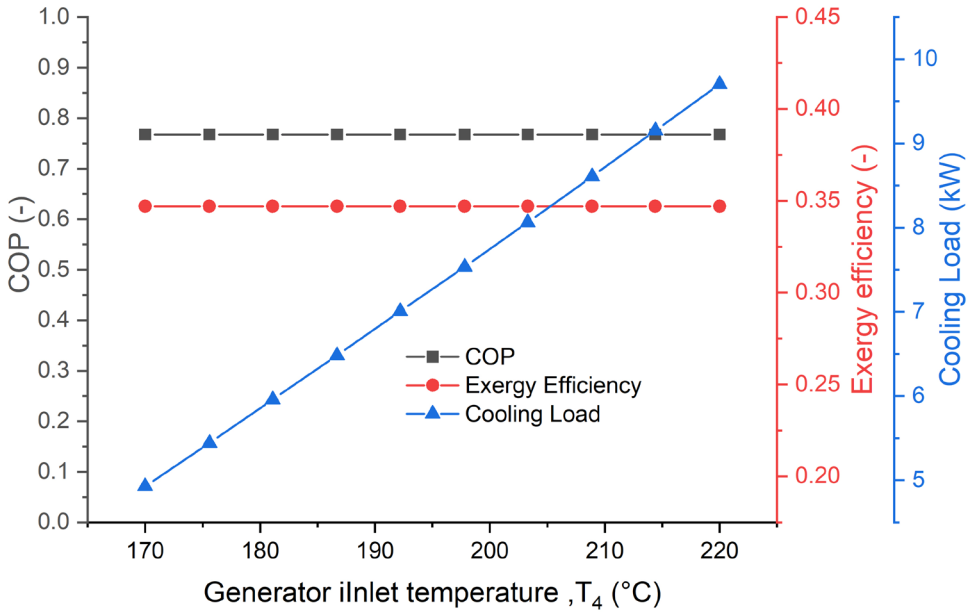

Figure 4.2. Effect of generator inlet temperature on COP, exergy efficiency, and cooling load in a solar absorption cooling system

Figure 4.3 demonstrates how the generator inlet temperature (T_4) influences key heat transfer rates in a solar absorption cooling system, including the $\dot{Q}_{Evap}$, $\dot{Q}_{abs}$, $\dot{Q}_{cond}$, $\dot{Q}_{Gen}$, and $\dot{Q}_{SHEX}$. As T_4 increases from 170°C to 220°C, all major heat transfer rates except $\dot{Q}_{SHEX}$ show a clear upward trend. The $\dot{Q}_{Evap}$ increases significantly, indicating enhanced cooling capacity at higher generator temperatures as more refrigerants are vaporized and circulated through the system. Similarly, the absorber heat transfer rate ($\dot{Q}_{abs}$) and condenser heat transfer rate ($\dot{Q}_{cond}$) experience an increase in heat rejection, which suggests a higher refrigerant flow rate and greater cooling power but also indicates a need for effective heat dissipation to maintain system stability. The generator heat input ($\dot{Q}_{Gen}$) rises proportionally with T_4, reflecting the additional thermal energy required to separate the refrigerant from the absorbent, highlighting the trade-off between increased cooling performance and higher energy demand. Interestingly, the $\dot{Q}_{SHEX}$ remains relatively low and shows only a slight increase, indicating a stable internal heat recovery process that prevents excessive energy losses.

While a higher T_4 improves system performance, it also raises the overall heat rejection in the condenser and absorber, necessitating efficient thermal management solutions such as larger heat exchangers or cooling towers.

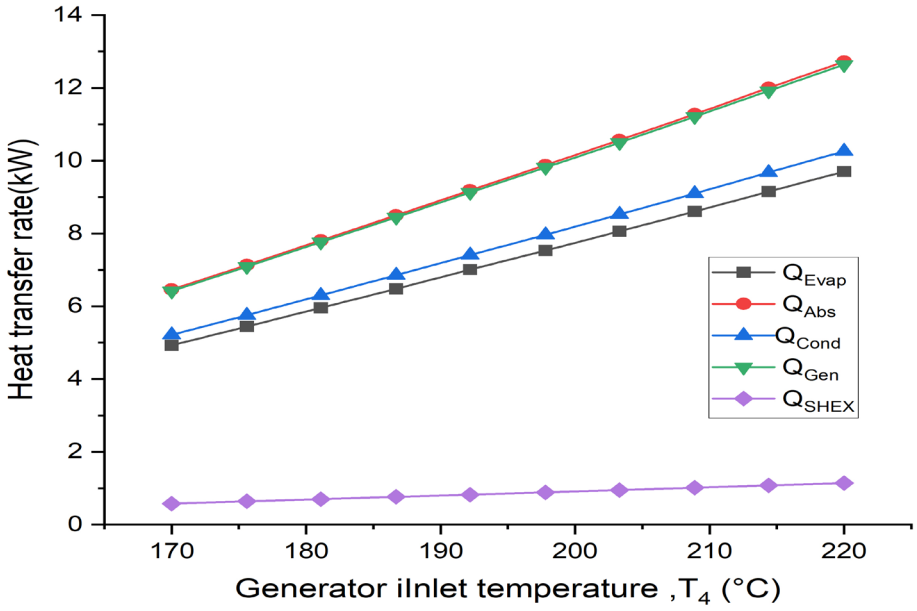

Figure 4.3. Effect of generator inlet temperature on heat transfer rates in a solar absorption cooling system

Figure 4.4 shows the impact of generator exit temperature (T_{10}) on three main performance parameters: COP, exergy efficiency, and cooling load. As T_{10} rises from around 70°C to 100°C. The results showed that Higher generator exit temperatures lead to reduced exergy efficiency and cooling load, with a slight negative effect on COP. The COP slightly declines, indicating a modest decrease in system efficiency at higher exit temperatures. This suggests that increasing T_{10} slightly lowers the cooling efficiency per unit of input energy. Exergy Efficiency sharply decreases with increasing generator exit temperature. The large drop indicates that higher generator temperatures cause greater irreversibilities and energy losses within the system. The system delivers slightly less cooling power ($\dot{Q}_{Cooling}$) at higher generator exit temperatures. It gradually declined with increasing T_{10}. from about 9.6 kW to ~8.6 kW. This may be due to thermodynamic limitations or reduced mass flow rates in the system components.

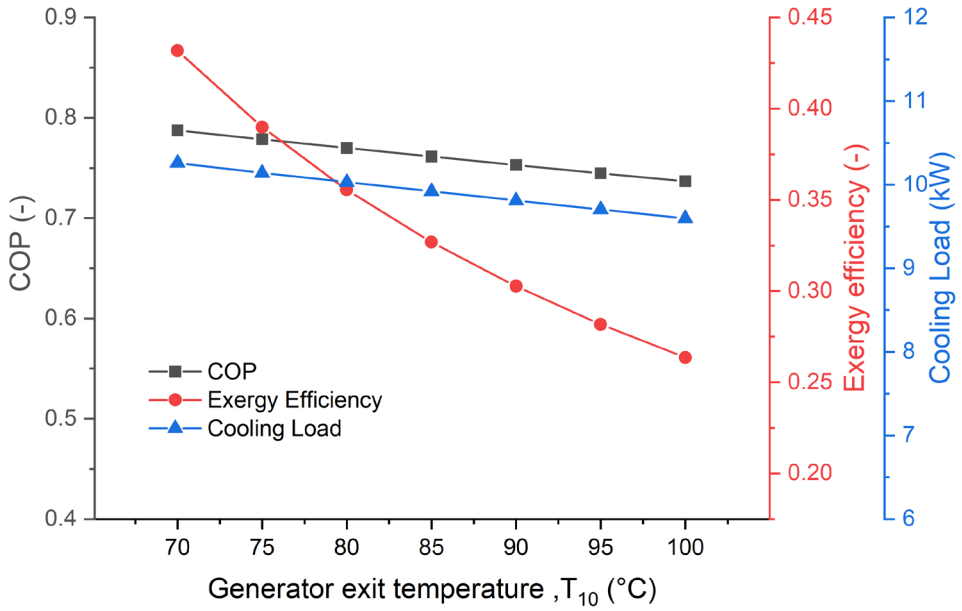

Figure 4.4. Effect of generator exit temperature on cop, exergy efficiency, and cooling load in a solar absorption cooling system.

Figure 4.5 illustrates how various heat transfer rates in the system respond to changes in the generator exit temperature (T_{10}), ranging from 70°C to 100°C. It appears from the findings that most heat transfer rates remain relatively stable, with minor trends suggesting moderate thermal sensitivity to generator exit temperature. $\dot{Q}_{SHEX}$ increases significantly compared to others, highlighting the growing role of the solution heat exchanger in energy recovery at higher temperatures. $\dot{Q}_{Evap}$ decreases slightly from ~10.4 kW to ~9.8 kW because Less cooling energy is absorbed at higher generator temperatures, consistent with the decline in cooling load seen in Figure 4.4. $\dot{Q}_{Gen}$ and $\dot{Q}_{Abs}$ show very slight increases, remaining nearly constant (~13.0–13.2 kW). The generator and absorber units maintain relatively stable heat exchange behavior, suggesting a balanced thermal loop unaffected by moderate increases in T_{10}. Also, $\dot{Q}_{Cond}$ Slight decrease, from ~11.0 kW to ~10.6 kW, likely due to changes in refrigerant mass flow or pressure conditions.

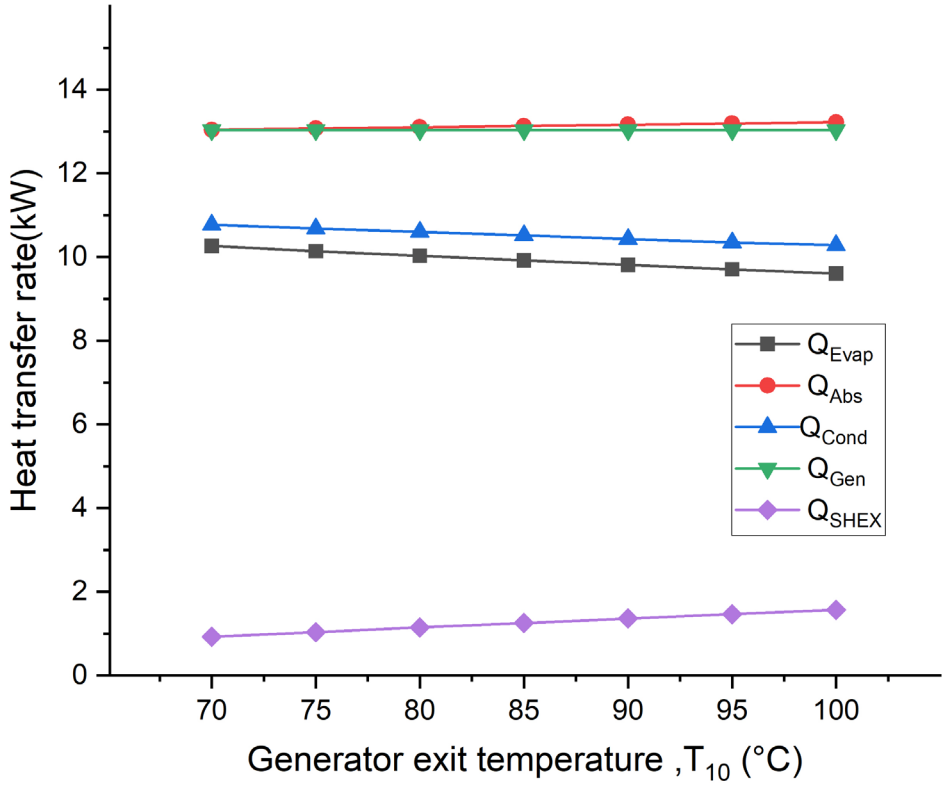

Figure 4.5. Effect of generator exit temperature on heat transfer rates in a solar absorption cooling system.

Figure 4.6 demonstrates the effect of direct normal irradiation (DNI) on the performance of a solar absorption cooling system and reveals that cooling load ($\dot{Q}_{Cooling}$) increases significantly with higher DNI, demonstrating a linear relationship between solar radiation intensity and the system's cooling capacity. As DNI rises from 400 W/m² to 800 W/m², the cooling load steadily increases, indicating that higher solar availability enhances system output, making it particularly effective in regions with strong solar exposure. However, despite this increase in cooling capacity, the COP remains nearly constant at around 0.75, suggesting that the system maintains a stable efficiency regardless of solar intensity. Similarly, exergy efficiency remains relatively unchanged (~35%), indicating that irreversibilities within the system are not significantly affected by variations in DNI, and the system's thermodynamic behavior remains consistent across different solar conditions.

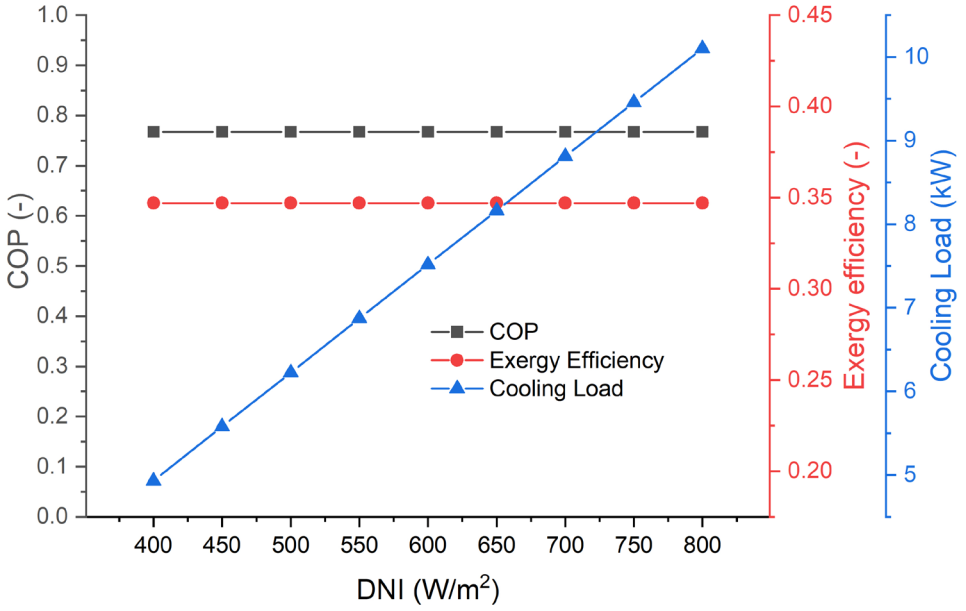

Figure 4.6. Effect of Direct Normal Irradiations (DNI) on COP, exergy efficiency, and cooling load in a solar absorption cooling system.

Figure 4.7 presents the heat transfer rates in a solar absorption cooling system as a function of DNI and demonstrates a direct relationship between solar radiation intensity and system performance. As DNI increases from 400 W/m² to 800 W/m², all heat transfer rates increase proportionally, with the $\dot{Q}_{Gen}$ and $\dot{Q}_{abs}$ reaching approximately 13.5 kW at 800 W/m², showing their dominant role in system energy exchange. Similarly, the $\dot{Q}_{Evap}$ and $\dot{Q}_{Cond}$ increase from around 5.5 kW at 400 W/m² to nearly 9.5 kW at 800 W/m², reflecting the growth in cooling capacity and heat rejection efficiency. In contrast, the $\dot{Q}_{SHEX}$ remains significantly lower, increasing slightly from 0.6 kW to 1.2 kW, indicating its limited contribution to overall heat transfer performance. These findings confirm that higher DNI significantly boosts system efficiency and cooling power, making solar radiation a key determinant of system effectiveness. To further enhance performance, optimizing the heat exchanger design in the generator, absorber, and condenser to improve thermal efficiency and integrating a thermal energy storage (TES) system can help store excess energy during peak DNI periods, ensuring continuous operation during low solar radiation conditions.

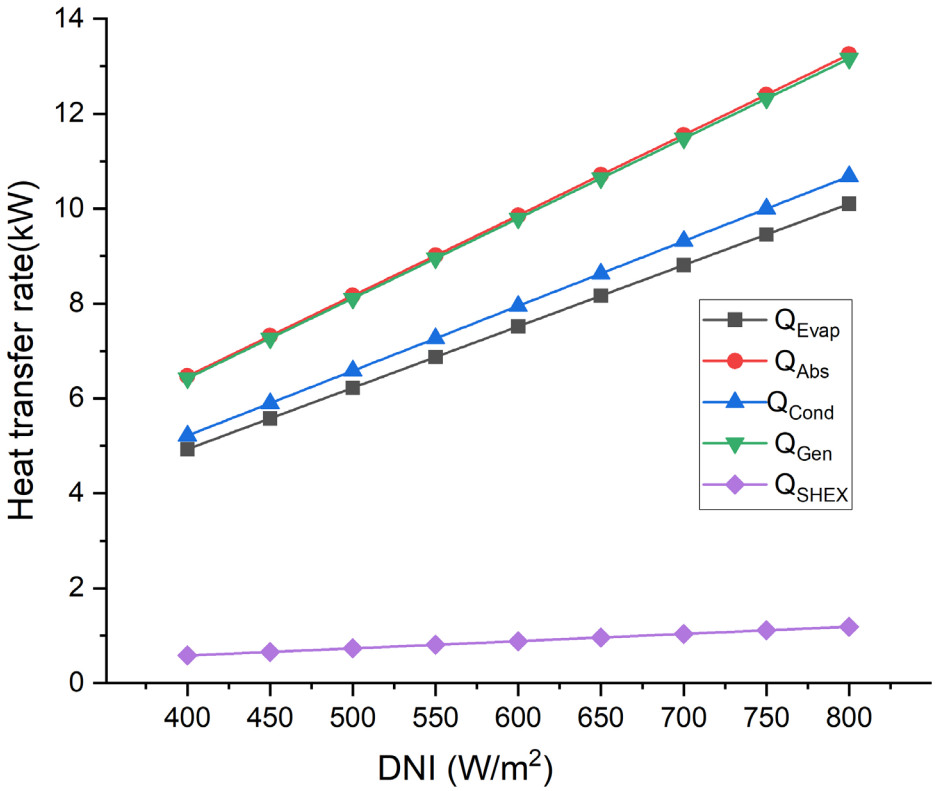

Figure 4.7. Effect of Direct Normal Irradiations (DNI) on heat transfer rates in a solar absorption cooling system.

Figure 9 presents the collector area effects on system performance, showing that as the collector area increases from 50 m² to 100 m², the cooling load rises significantly from approximately 2.5 kW to 14 kW, demonstrating a direct correlation between solar energy collection and cooling capacity. However, despite this increase in cooling output, the COP remains stable at around 0.75, indicating that system efficiency does not improve with a larger collector area but maintains a consistent cooling-to-energy input ratio. Similarly, exergy efficiency stays constant at approximately 35%.

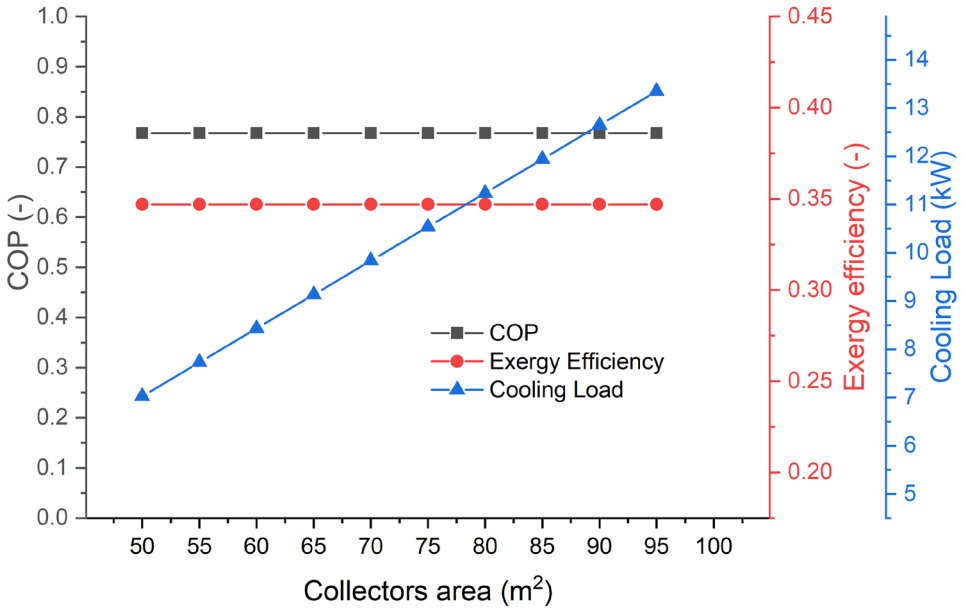

Figure 4.8. Effect of Collectors Area on COP, exergy efficiency, and cooling load in a solar absorption cooling system.

Figure 4.9 illustrates the analysis of collector area effects on heat transfer rates in a solar absorption cooling system, revealing that increasing the collector area from 50 m² to 100 m² significantly enhances system thermal performance, with all major heat transfer rates showing a proportional increase. The $\dot{Q}_{Gen}$ and $\dot{Q}_{abs}$ exhibit the highest heat transfer rates, rising from approximately 10 kW at 50 m² to nearly 17 kW at 100 m², demonstrating their dominant role in the absorption cooling. Similarly, the $\dot{Q}_{Evap}$ and $\dot{Q}_{Cond}$ increase from about 7 kW to 13 kW, ensuring balanced cooling and heat rejection as more solar energy is collected. The findings also present that $\dot{Q}_{SHEX}$ slight increase with collector area from ~0.9 kW to ~1.5 kW. The solution heat exchanger plays a secondary but consistent role. Its performance improves modestly with more solar energy available but remains the smallest among all heat rates.

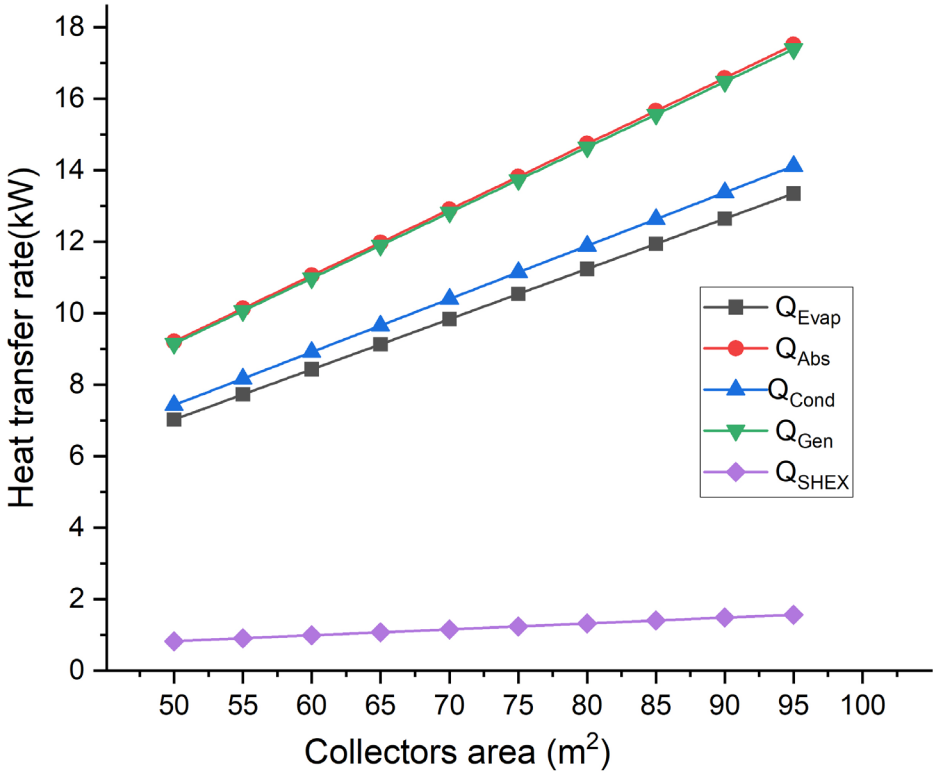

Figure 4.9. Effect of collectors area on heat transfer rates in a solar absorption cooling system.

Figure 4.10 illustrates the impact of varying evaporator temperatures (from -3°C to 6°C) on three key performance parameters in a solar absorption cooling system: COP, exergy efficiency, and cooling load. The figure reveals that COP alone is not a sufficient system performance indicator, as it remains stable while exergy efficiency declines significantly. Although the cooling load remains relatively unaffected, the exergy analysis reveals substantial performance degradation with increased evaporator temperature. COP remains nearly constant, with a very slight upward trend from around 0.74 to 0.76. A marginal increase suggests a minor improvement in thermal efficiency as the evaporator temperature increases, possibly due to a reduced temperature lift (difference between evaporator and condenser temperatures), which lowers the system's energy demand. Exergy efficiency strongly decreases with increasing evaporator temperatures from approximately 0.50 at -3°C to 0.33 at 6°C. The system experiences greater irreversibility and exergy losses at higher evaporator temperatures. Cooling load is nearly constant across the range, with a slight downward slope. It Varies slightly from 10.1 to 9.9 kW. This can be attributed to a reduced

temperature gradient between the evaporator and the cooled space, decreasing the heat absorption rate.

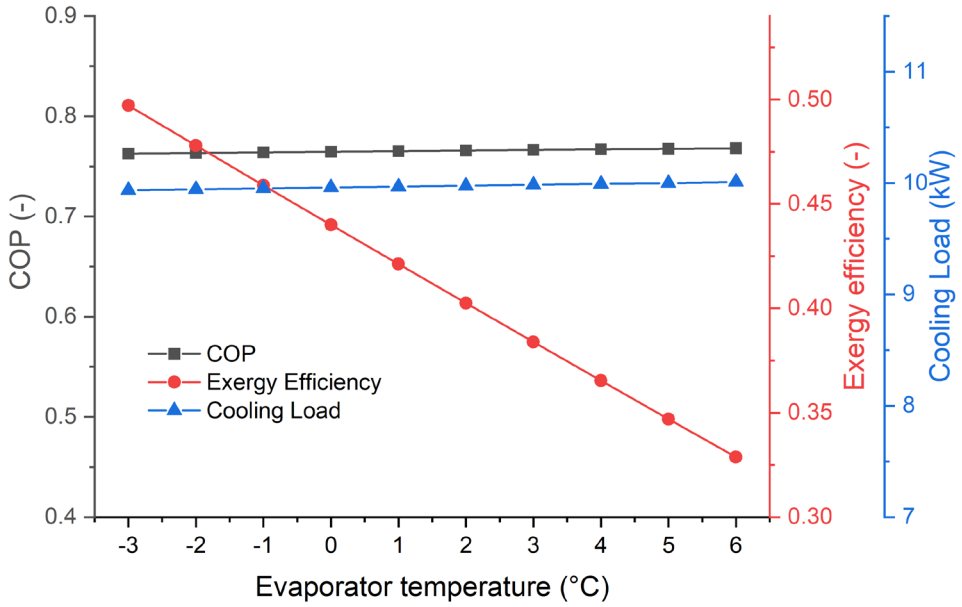

Figure 4.10. Effect of evaporator temperature on COP, exergy efficiency, and cooling load in a solar absorption cooling system.

Figure 4.11 illustrates how variations in evaporator temperature (ranging from -3°C to +6°C) affect heat transfer rates in five major solar absorption cooling system components. The figure shows that all heat transfer rates remain remarkably stable across the evaporator temperature ranges. The generator, absorber, condenser, and solution heat exchanger demonstrate thermal resilience and minimal sensitivity to the evaporator temperature. The slight drop in $\dot{Q}_{Evap}$ is consistent with reduced driving temperature differences as the evaporator temperature increases. $\dot{Q}_{Evap}$ is almost constant, with a very slight downward slope between 10.0 and 9.8 kW, as the heat absorbed by the evaporator decreases slightly as its temperature rises. $\dot{Q}_{Abs}$ and $\dot{Q}_{Gen}$ remain almost constant across the temperature range. Both are around 13.0 kW, as the evaporator temperature does not significantly affect these components. $\dot{Q}_{Cond}$ is also constant, around 10.8 kW. Like the absorber and generator, the condenser heat rejection is unaffected by the variation in evaporator temperature. $\dot{Q}_{SHEX}$ constant at ~1.2 kW. The solution heat exchanger remains unaffected by evaporator temperature,

primarily facilitating internal energy recovery between strong and weak solutions. Its operation depends more on solution properties and generator temperature than evaporator conditions.

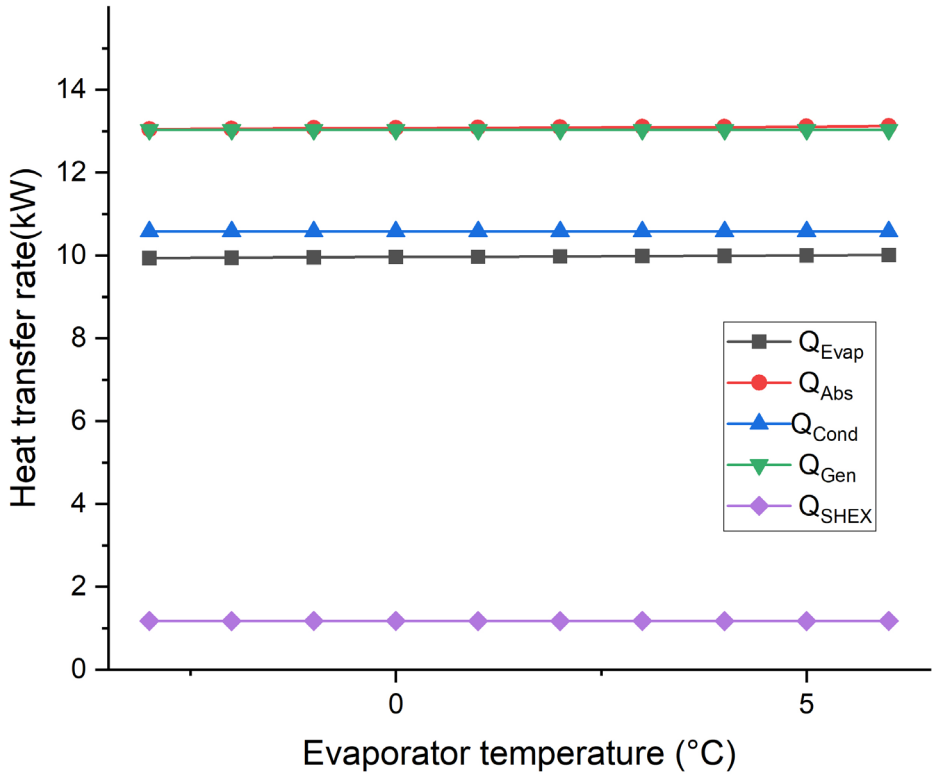

Figure 4.11. Effect of evaporator temperature on heat transfer rates in a solar absorption cooling system.

Figure 4.12 demonstrates how increasing the effectiveness of the Solution Heat Exchanger (SHEX) influences three critical performance parameters in a solar-driven absorption cooling system: COP, Exergy Efficiency, and Cooling Load. The SHEX effectiveness varies from 0.40 to 0.75, representing an improvement in internal energy recovery within the absorption cycle. The figure shows that all three-performance metrics significantly improve with rising SHEX effectiveness. COP steady linear increase with SHEX effectiveness from approximately 0.72 at 0.40 effectiveness to 0.85 at 0.75 effectiveness. This reduces the required external heat input in the generator, improving thermal efficiency and resulting in a higher COP. Exergy efficiency gradually increases from ~0.59 to ~0.68. Enhanced SHEX effectiveness reduces entropy generation and irreversibilities, boosting the exergy (second-law)

efficiency. Also, the Cooling load has a significant upward trend, increasing from ~9.0 kW to ~11.5 kW. Improved SHEX effectiveness results in more efficient thermal distribution and less energy loss within the cycle, enabling the system to deliver more cooling output. This indicates that the SHEX doesn't just reduce generator demand—it also enhances the evaporator's capacity to absorb heat.

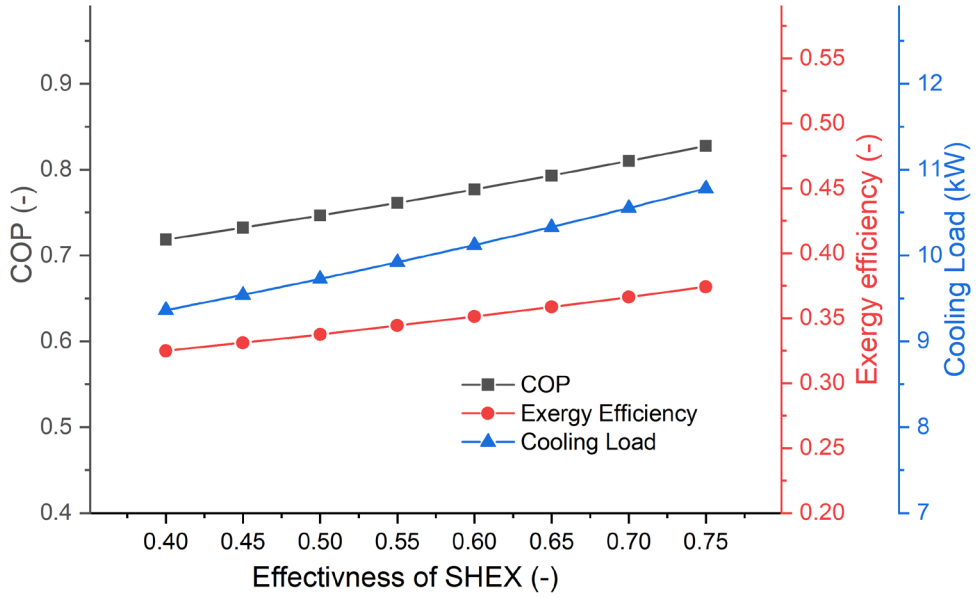

Figure 4.12. Effect of effectiveness of SHEX on COP, exergy efficiency, and cooling load in a solar absorption cooling system.

Figure 4.13 presents the impact of the effectiveness of the SHEX on heat transfer rates in a solar absorption cooling system. Increasing SHEX effectiveness from 0.40 to 0.75 significantly improves system performance, particularly in cooling capacity and heat recovery efficiency. The $\dot{Q}_{Evap}$ and $\dot{Q}_{Cond}$ increase from approximately 9.5 kW to 11 kW, confirming that a more efficient SHEX enhances cooling output and heat rejection capacity. Meanwhile, the generator $\dot{Q}_{Gen}$ and $\dot{Q}_{abs}$ maintain relatively stable heat transfer rates of around 13.5 kW, indicating that the primary effect of SHEX optimization is on the cooling side rather than the heat generation processes. The most notable improvement is seen in $\dot{Q}_{SHEX}$, which rises sharply from around 0.6 kW to nearly 1.5 kW, demonstrating that a more effective SHEX significantly enhances internal energy recovery, reducing thermal losses and improving exergy efficiency.

These results highlight that optimizing SHEX beyond 0.70 can maximize cooling capacity, lower entropy generation, and increase overall system sustainability.

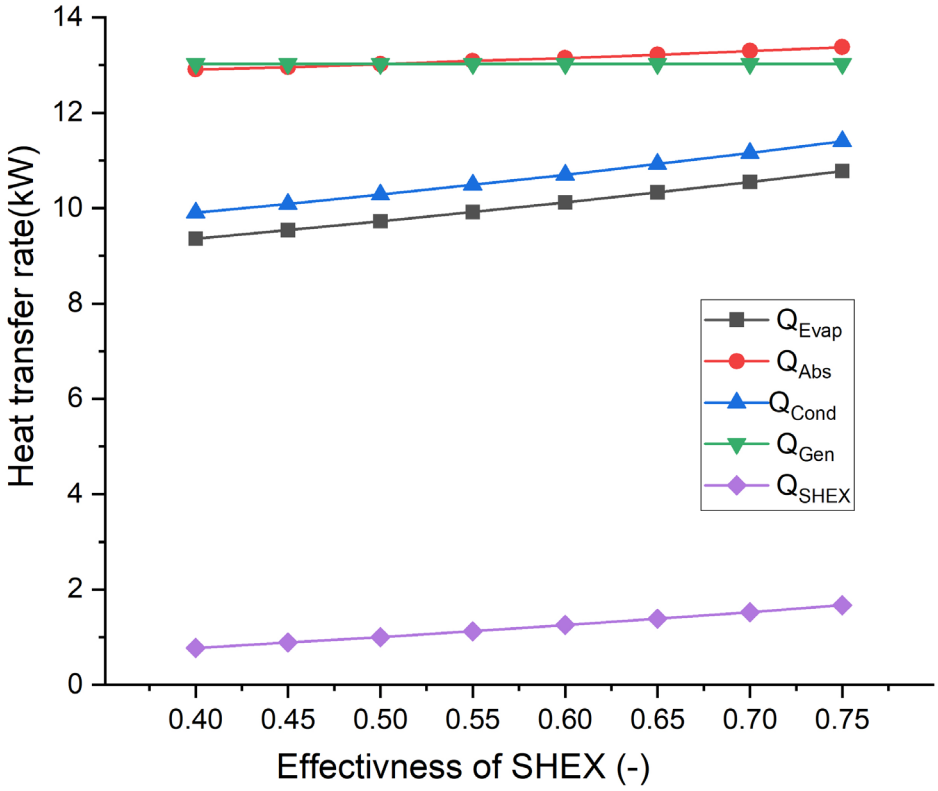

Figure 4.13. Effect of effectiveness of SHEX on heat transfer rates in a solar absorption cooling system.

4.4. SEASONAL AND OPERATIONAL IMPACTS ON SOLAR ABSORPTION COOLING SYSTEM PERFORMANCE IN LIBYAN CITIES

Figure 4.14 illustrates the analysis of DNI variation in Tripoli, Benghazi, and Misrata. It reveals a clear seasonal trend, with peak DNI values occurring between May and July, reaching approximately 850 W/m² in Benghazi, 830 W/m² in Tripoli and 780 W/m² in Misrata, indicating the optimal period for solar energy generation. Conversely, the lowest DNI levels are observed from November to January, dropping below 400 W/m², highlighting the need for hybrid solar systems to maintain energy supply during low-radiation months. Benghazi consistently records the highest DNI, making it the most suitable location for solar power projects, followed by Tripoli and

Misrata, which receive slightly lower radiation levels due to geographical and atmospheric differences.

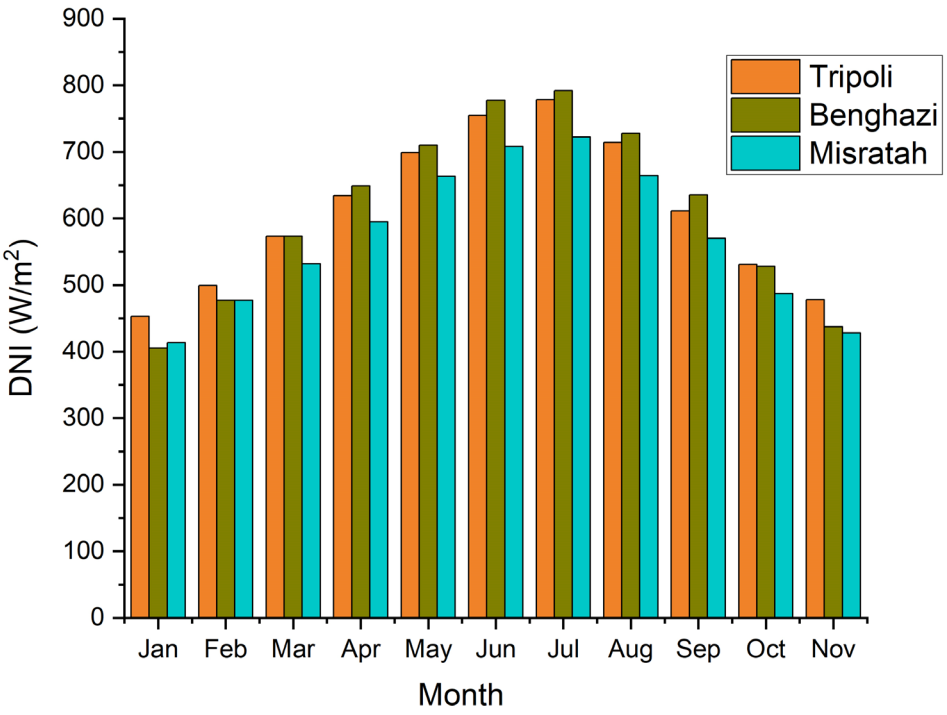

Figure 4.14. Monthly variation of DNI in Tripoli, Benghazi, and Misrata

The bar chart in Figure 4.15 illustrates the monthly cooling load variation (kW) in Tripoli, Benghazi, and Misrata, showing a clear seasonal pattern that correlates with temperature variations and solar radiation intensity. The cooling demand gradually increases from January to June, peaking during summer (June–July) when the cooling load exceeds 10 kW in Benghazi, slightly lower in Tripoli, and the lowest in Misrata. This trend aligns with higher ambient temperatures and increased solar radiation during summer, requiring greater cooling demand to maintain indoor thermal comfort. The cooling load starts declining from August onward, reaching its lowest level between November and January (approximately 5 kW), as temperatures decrease and the need for cooling diminishes.

Benghazi consistently exhibits the highest cooling load among the three cities, likely due to higher DNI values and slightly warmer conditions than Tripoli and Misrata. Tripoli follows closely, while Misrata has the lowest cooling demand, indicating

possible differences in urban heat island effects, humidity levels, and building insulation characteristics. These findings suggest that solar absorption cooling systems should be designed with higher capacities for summer months, and TES or hybrid cooling systems can help maintain efficiency during seasonal cooling variations.

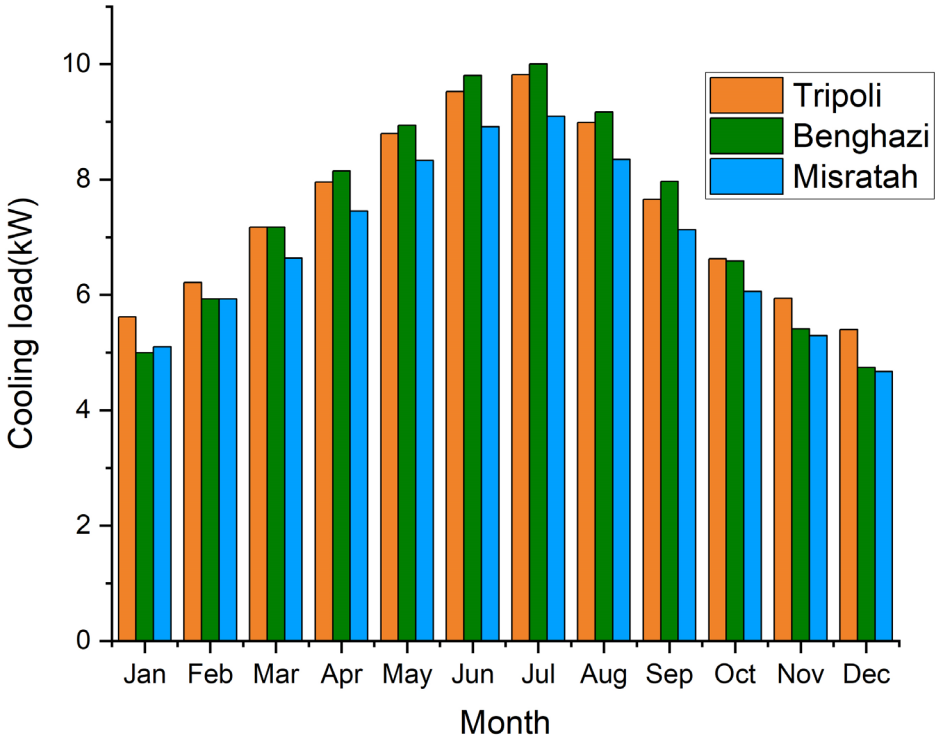

Figure 4.15. Monthly variation of cooling load in Tripoli, Benghazi, and Misrata

Figure 4.16 presents the monthly solar coefficient of performance (SCOP) for three Libyan cities: Tripoli (orange), Benghazi (green), and Misrata (blue) over a full calendar year (January to December).

The figure shows that SCOP values for all three cities remain within a narrow range of approximately 0.41 to 0.43 throughout the year. The highest SCOP values are observed from May to August, indicating better system efficiency during the summer months. The lowest SCOP values appear in January, February, and December, reflecting seasonal variation and reduced solar energy availability in winter. Tripoli generally shows the highest SCOP across most months. This can be attributed to its coastal location, high solar radiation, and relatively warmer temperatures throughout

the year. Benghazi follows Tripoli closely and shows slightly lower SCOP values. Although also coastal, Benghazi is located further east and may receive slightly different solar profiles. Misrata consistently exhibits the lowest SCOP values of the three cities, though still within a close margin.

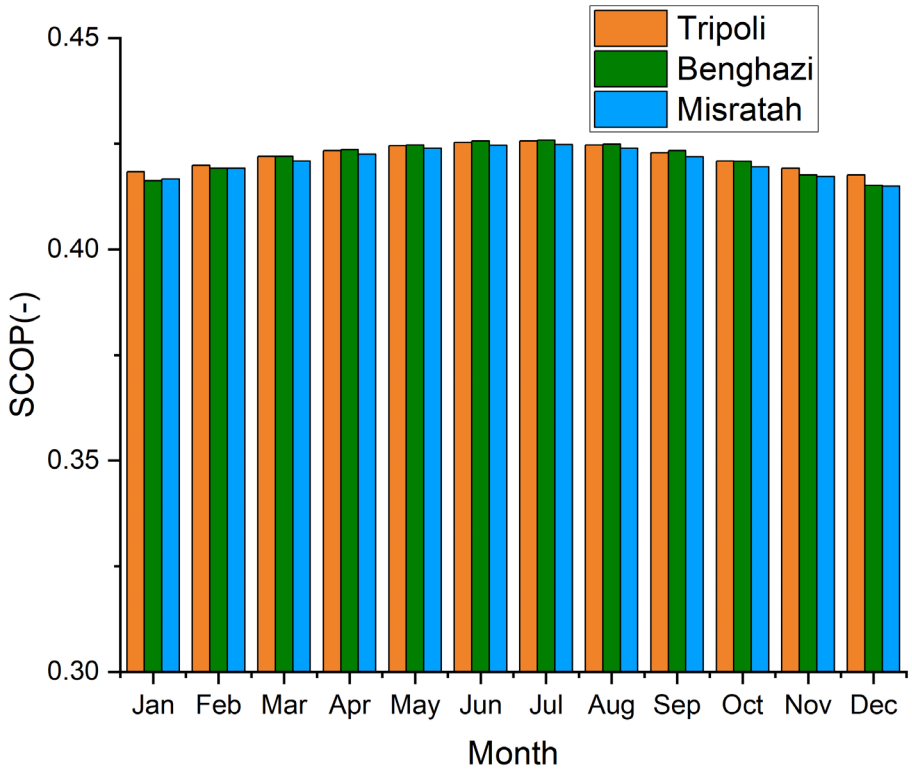

Figure 4.16. Monthly Variation of Solar Coefficient of Performance (SCOP) in Tripoli, Benghazi, and Misrata.

Figure 4.17 presents the monthly generator heat transfer rate (kW) for three Libyan cities, Tripoli, Benghazi, and Misrata, over a full calendar year (January to December). The Figure illustrates that the generator heat transfer rate varies significantly throughout the year, peaking in summer and declining in winter, in line with solar irradiance cycles. Tripoli maintains a marginal performance advantage over Benghazi and Misrata. The generator heat transfer rate exhibits a clear seasonal pattern, increasing from January to July, peaking in July, and then decreasing until December. The lowest generator heat transfer rates were observed during the winter months (January–February) (approximately 6.5–7.5 kW) due to lower solar energy availability. A strong upward trend was observed from spring to summer (March–

July); by July, rates peaked (approximately 13.5–14.2 kW). In autumn (August–December), the rate gradually decreased to winter levels, as a result of lower solar energy input. Tripoli has the highest generator heat transfer rate compared to Benghazi and Misrata in Winter (Jan–Mar and Nov–Dec). Indicates better winter solar availability or collector performance in Tripoli. Benghazi and Misrata cities show higher generator heat transfer rates than Tripoli in Summer (May–Aug). Misrata generally leads, especially in July, indicating strong summer solar input. Benghazi and Misrata benefit from better collector performance or clearer skies in the summer months.

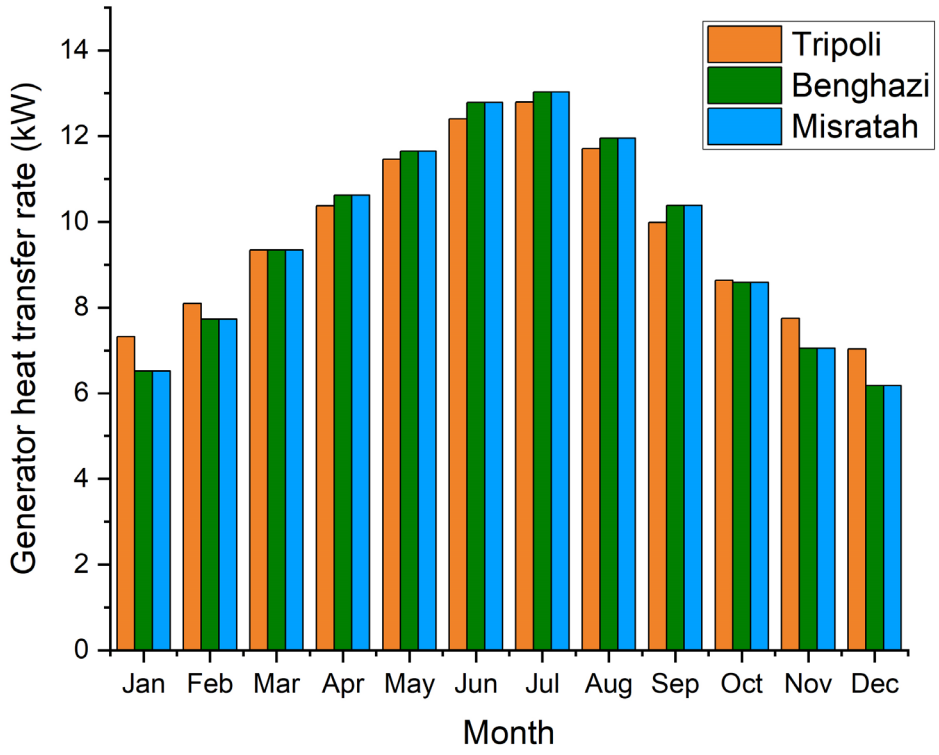

Figure 4.17. Monthly Variation of Solar Coefficient of Performance (SCOP) in Tripoli, Benghazi, and Misrata.

CHAPTER 5

CONCLUSION

This study comprehensively evaluated the thermodynamic, exergy, and thermo-economic performance of a solar-driven absorption cooling system designed for Tripoli, Benghazi, and Misrata, Libya. By integrating parabolic trough collectors (PTC) with a lithium bromide-water ($LiBr-H_2O$) absorption refrigeration cycle, the system effectively utilizes solar energy to meet cooling demands while minimizing reliance on fossil fuels. The results indicate that DNI, generator inlet temperature, evaporator temperature, and collector area significantly impact system performance metrics such as COP, exergy efficiency, cooling load, and heat transfer rates. Increasing DNI and collector area enhances cooling capacity, with the cooling load rising from 2.5 kW to 14 kW as the collector area expands from 50 m^2 to 100 m^2. Additionally, increasing the generator inlet temperature improves cooling output while maintaining a COP of ~0.75–0.8, demonstrating efficient heat utilization. However, exergy efficiency decreases as evaporator temperature rises, dropping from 80% to 32% between -3°C and 6°C, indicating the need to balance system parameters for optimal efficiency. The findings suggest integrating thermal energy storage (TES) and hybrid solar-PV configurations can enhance system reliability, particularly during low-solar-radiation periods. Future work should focus on real-world implementation, advanced storage technologies, and hybrid system configurations to maximize efficiency and economic feasibility in high-irradiation regions.

Summary of Main Results:

- Increasing DNI and collector area significantly improves cooling performance, with cooling load rising from 2.5 kW to 14 kW as the collector area expands from 50 m^2 to 100 m^2.

- Higher generator inlet temperature enhances cooling output while maintaining COP (~0.75–0.8), confirming efficient heat utilization.
- Exergy efficiency declines from 80% to 32% as evaporator temperature increases from -3°C to 6°C, highlighting the need for optimal parameter selection.
- Tripoli consistently exhibits higher generator heat transfer rates, making it the most suitable location for solar-driven cooling applications.
- Thermal energy storage (TES) integration is crucial for maintaining system efficiency during periods of low solar radiation.
- Future improvements should focus on hybrid solar-PV integration, enhanced heat exchanger designs, and real-world system validation to ensure long-term sustainability and economic feasibility.

Future Work

Future research should focus on experimental validation of the proposed system under real-world operating conditions to compare simulation results with practical performance. Additionally, further optimization of the thermodynamic and economic parameters can enhance system feasibility for large-scale deployment. Integrating advanced thermal energy storage (TES) solutions, such as phase-change materials (PCMs) or hybrid PV-thermal systems, could further improve efficiency and sustainability. A techno-economic analysis for different geographical locations with varying climate and solar resource availability is also essential to assess system adaptability. Moreover, incorporating machine learning-based predictive control strategies could optimize system operation by adjusting parameters in real time based on solar availability and cooling demand. Finally, exploring the potential of waste heat recovery and multi-generation systems could enhance overall energy utilization and further reduce reliance on conventional cooling technologies.

REFERENCES

1. Waite, M., Cohen, E., Torbey, H., Piccirilli, M., Tian, Y., and Modi, V., "Global trends in urban electricity demands for cooling and heating", ***Energy***, 127: 786–802 (2017).

2. Omer, A. M., "Energy, environment and sustainable development", ***Renewable And Sustainable Energy Reviews***, 12 (9): 2265–2300 (2008).

3. Akroot, A. and Refaei, M., "Thermodynamic and Exergoeconomic Assessment of a Solar-Assisted Combined Cooling, Heating, and Power System in Antalya, Turkey", ***Gazi Üniversitesi Fen Bilimleri Dergisi Part C: Tasarım Ve Teknoloji***, 1 (2025).

4. Mekhilef, S., Saidur, R., and Safari, A., "A review on solar energy use in industries", ***Renewable And Sustainable Energy Reviews***, 15 (4): 1777–1790 (2011).

5. Dawood, T. A., Raphael, R., Barwari, I., and Akroot, A., "Solar Energy and Factors Affecting the Efficiency and Performance of Panels in Erbil / Kurdistan", ***International Journal Of Heat And Technology***, 41 (2): 304–312 (2023).

6. Kurkute, N. and Priyam, A., .

7. Šujanová, P., Rychtáriková, M., Sotto Mayor, T., and Hyder, A., "A healthy, energy-efficient and comfortable indoor environment, a review", ***Energies***, 12 (8): 1414 (2019).

8. Spengler, J. D. and Chen, Q., "Indoor air quality factors in designing a healthy building", ***Annual Review Of Energy And The Environment***, 25 (1): 567–600 (2000).

9. Hu, M., "Indoor Environmental Impact on Human Health", Smart Technologies and Design For Healthy Built Environments, ***Springer International Publishing***, Cham, 57–74 (2021).

10. D'Ambrosio Alfano, F. R., Olesen, B. W., Palella, B. I., and Riccio, G., "Thermal comfort: Design and assessment for energy saving", ***Energy And Buildings***, 81: 326–336 (2014).

11. Fantozzi, F. and Rocca, M., "An extensive collection of evaluation indicators to assess occupants' health and comfort in indoor environment", ***Atmosphere***, 11 (1): 90 (2020).

12. Qu, M., Liu, X., Yang, Z., Wu, F., Shi, L., Liu, X., Zhang, T., Liu, X., Jiang, Y., and Yin, H., "Energy-saving technologies for building heating, ventilation, and air conditioning systems", ***Annual Review Of Heat Transfer***, 21: (2018).

13. Baus, L. and Nehr, S., "Potentials and limitations of direct air capturing in the built environment", ***Building And Environment***, 208: 108629 (2022).

14. Litardo, J., Gomez, D., Boero, A., Hidalgo-Leon, R., Soriano, G., and Ramirez, A. D., "Air-conditioning life cycle assessment research: a review of the methodology, environmental impacts, and areas of future improvement", ***Energy And Buildings***, 296: 113415 (2023).

15. Kılıç, M., "Evaluation of combined thermal–mechanical compression systems: A review for energy efficient sustainable cooling", ***Sustainability***, 14 (21): 13724 (2022).

16. Mishra, A., Alam, M. I., Pal, D. B., and Awasthi, S., "Solar Energy and Its Utilization in Smart Cities", Renewable Energy Development: Technology, Material and Sustainability, ***Springer Nature Singapore***, Singapore, 111–131 (2025).

17. Abbasi, T. and Abbasi, S. A., "Biomass energy and the environmental impacts associated with its production and utilization", ***Renewable And Sustainable Energy Reviews***, 14 (3): 919–937 (2010).

18. Hasan, M. M., Hossain, S., Mofijur, M., Kabir, Z., Badruddin, I. A., Yunus Khan, T. M., and Jassim, E., "Harnessing solar power: a review of photovoltaic innovations, solar thermal systems, and the dawn of energy storage solutions", ***Energies***, 16 (18): 6456 (2023).

19. Ehtiwesh, I. A. S., Neto Da Silva, F., and Sousa, A. C. M., "Deployment of parabolic trough concentrated solar power plants in North Africa–a case study for Libya", ***International Journal Of Green Energy***, 16 (1): 72–85 (2019).

20. Rashid, F. L., Eleiwi, M. A., Mohammed, H. I., Ameen, A., and Ahmad, S., "A review of using solar energy for cooling systems: applications, challenges, and effects", ***Energies***, 16 (24): 8075 (2023).

21. Bassam, N. El, "Solar energy: Technologies and options", ***Distributed Renewable Energies For Off-Grid Communities: Empowering A Sustainable, Competitive, And Secure Twenty-First Century***, 123–147 (2021).

22. Akroot, A., Almaktar, M., and Alasali, F., "The Integration of Renewable Energy into a Fossil Fuel Power Generation System in Oil-Producing Countries: A Case Study of an Integrated Solar Combined Cycle at the Sarir Power Plant", ***Sustainability (Switzerland)*** , 16 (11): (2024).

23. Akroot, A. and Al Shammre, A. S., "Techno-Economic and Environmental Impact Analysis of a 50 MW Solar-Powered Rankine Cycle System", ***Processes***, 12 (6): 1059 (2024).

24. Ahmad, A., Prakash, O., Kausher, R., Kumar, G., Pandey, S., and Hasnain, S. M. M., "Parabolic trough solar collectors: A sustainable and efficient energy source", ***Materials Science For Energy Technologies***, 7 (August 2023): 99–106 (2024).

25. Bellos, E., Tzivanidis, C., and Antonopoulos, K. A., "A detailed working fluid investigation for solar parabolic trough collectors", ***Applied Thermal Engineering***, 114: 374–386 (2017).

26. Cabrera, F. J., Fernández-García, A., Silva, R. M. P., and Pérez-García, M., "Use of parabolic trough solar collectors for solar refrigeration and air-conditioning applications", ***Renewable And Sustainable Energy Reviews***, 20: 103–118 (2013).

27. Kamran, M., "Energy sources and technologies", ***Fundamentals Of Smart Grid Systems***, 23–69 (2023).

28. Jebasingh, V. K. and Herbert, G. M. J., "A review of solar parabolic trough collector", ***Renewable And Sustainable Energy Reviews***, 54: 1085–1091 (2016).

29. Talal, W. and Akroot, A., "An Exergoeconomic Evaluation of an Innovative Polygeneration System Using a Solar-Driven Rankine Cycle Integrated with the Al-Qayyara Gas Turbine Power Plant and the Absorption Refrigeration Cycle", ***Machines***, 12 (2): 133 (2024).

30. Alfaris, A., Akroot, A., Alqaed, S., and Almehmadi, F. A., "Performance analysis of integrated solar and natural gas combined cycle power plants in high solar potential regions", ***Scientific Reports***, 15 (1): 9181 (2025).

31. Guercio, A., Curto, D., Franzitta, V., Frascati, M., Milone, D., Martorana, P., and Mantegna, M., "Energy Analyses and Optimization Proposals for Hotels in Sicily: A Case Study", ***Sustainability***, 16 (1): 146 (2023).

32. Awasthi, A., Shukla, A. K., Murali Manohar, S. R., Dondariya, C., Shukla, K. N., Porwal, D., and Richhariya, G., "Review on sun tracking technology in solar PV system", ***Energy Reports***, 6: 392–405 (2020).

33. Kılıç, M., "Evaluation of combined thermal–mechanical compression systems: A review for energy efficient sustainable cooling", ***Sustainability***, 14 (21): 13724 (2022).

34. Ayou, D. S. and Coronas, A., "New developments and progress in absorption chillers for solar cooling applications", ***Applied Sciences***, 10 (12): 4073 (2020).

35. Shirazi, A., Taylor, R. A., Morrison, G. L., and White, S. D., "Solar-powered absorption chillers: A comprehensive and critical review", ***Energy Conversion And Management***, 171: 59–81 (2018).

36. Dokhaee, E., Saraei, A., Mohsenimonfared, H., and Yousefi, P., "Exergy and thermoeconomic analysis of a combined Allam generation system and absorption cooling system", ***International Journal Of Energy And Environmental Engineering***, 13 (1): 267–273 (2022).

37. Shirazi, A., Taylor, R. A., Morrison, G. L., and White, S. D., "Solar-powered absorption chillers: A comprehensive and critical review", ***Energy Conversion And Management***, 171: 59–81 (2018).

38. Soussi, M., Balghouthi, M., Guizani, A. A., and Bouden, C., "Model performance assessment and experimental analysis of a solar assisted cooling system", ***Solar Energy***, 143: 43–62 (2017).

39. Musbah, M. H., Z˘Ivković, B. D., Kosi, F. F., Abdulgalil, M. M., and Sretenović, A. A., "Solar energy contribution to the energy demand for air conditioning system in an office building under Tripoli climate conditions", ***Thermal Science***, 18: S1–S12 (2014).

40. Wrobel, J., Sanabria Walter, P., and Schmitz, G., "Performance of a solar assisted air conditioning system at different locations", ***Solar Energy***, 92: 69–83 (2013).

41. Baniyounes, A. M., Ghadi, Y. Y., Rasul, M. G., and Khan, M. M. K., "An overview of solar assisted air conditioning in Queensland's subtropical regions, Australia", ***Renewable And Sustainable Energy Reviews***, 26: 781–804 (2013).

42. Gude, V. G. and Nirmalakhandan, N., "Combined desalination and solar-assisted air-conditioning system", ***Energy Conversion And Management***, 49 (11): 3326–3330 (2008).

43. Ma, Y., Saha, S. C., Miller, W., and Guan, L., "Comparison of different solar-assisted air conditioning systems for Australian office buildings", ***Energies***, 10 (10): 1463 (2017).

44. Ibrahim, N. I., Al-Sulaiman, F. A., Rehman, S., Saat, A., and Ani, F. N., "Economic analysis of a novel solar-assisted air conditioning system with integral absorption energy storage", ***Journal Of Cleaner Production***, 291: 125918 (2021).

45. Ha, Q. P. and Vakiloroaya, V., "A Novel Solar-Assisted Air-Conditioner System for Energy Savings with Performance Enhancement", ***Procedia Engineering***, 49: 116–123 (2012).

46. Akyüz, A., Yıldırım, R., Gungor, A., and Tuncer, A. D., "Experimental investigation of a solar-assisted air conditioning system: Energy and life cycle climate performance analysis", ***Thermal Science And Engineering Progress***, 43: 101960 (2023).

47. Al-Ugla, A. A., El-Shaarawi, M. A. I., Said, S. A. M., and Al-Qutub, A. M., "Techno-economic analysis of solar-assisted air-conditioning systems for

commercial buildings in Saudi Arabia", ***Renewable And Sustainable Energy Reviews***, 54: 1301–1310 (2016).

48. Aguilar-Jiménez, J. A., Velázquez, N., López-Zavala, R., González-Uribe, L. A., Beltrán, R., and Hernández-Callejo, L., "Simulation of a solar-assisted air-conditioning system applied to a remote school", ***Applied Sciences***, 9 (16): 3398 (2019).

49. Baniyounes, A. M., Rasul, M. G., and Khan, M. M. K., "Assessment of solar assisted air conditioning in Central Queensland's subtropical climate, Australia", ***Renewable Energy***, 50: 334–341 (2013).

50. Rosiek, S. and Batlles Garrido, F. J., "Performance evaluation of solar-assisted air-conditioning system with chilled water storage (CIESOL building)", ***Energy Conversion And Management***, 55: 81–92 (2012).

51. Ren, H., Sun, Y., Albdoor, A. K., Tyagi, V. V., Pandey, A. K., and Ma, Z., "Improving energy flexibility of a net-zero energy house using a solar-assisted air conditioning system with thermal energy storage and demand-side management", ***Applied Energy***, 285: 116433 (2021).

52. Rosiek, S., "Exergy analysis of a solar-assisted air-conditioning system: Case study in southern Spain", ***Applied Thermal Engineering***, 148: 806–816 (2019).

53. Chen, E., Chen, J., Jia, T., Zhao, Y., and Dai, Y., "A solar-assisted hybrid air-cooled adiabatic absorption and vapor compression air conditioning system", ***Energy Conversion And Management***, 250: 114926 (2021).

54. Vakiloroaya, V., Ha, Q. P., and Skibniewski, M., "Modeling and experimental validation of a solar-assisted direct expansion air conditioning system", ***Energy And Buildings***, 66: 524–536 (2013).

55. Habib, M. F., Ali, M., Sheikh, N. A., Badar, A. W., and Mehmood, S., "Building thermal load management through integration of solar assisted absorption and desiccant air conditioning systems: A model-based simulation-optimization approach", ***Journal Of Building Engineering***, 30: 101279 (2020).

56. Rahman, A., Abas, N., Dilshad, S., and Saleem, M. S., "A case study of thermal analysis of a solar assisted absorption air-conditioning system using R-410A for domestic applications", ***Case Studies In Thermal Engineering***, 26: 101008 (2021).

57. Chen, E., Zhao, Y., Wang, M., Bian, M., Cai, W., Li, B., and Dai, Y., "Experimental investigation of a solar-assisted absorption-compression system for heating and cooling", ***Solar Energy***, 257: 18–33 (2023).

58. Hidalgo, M. C. R., Aumente, P. R., Millán, M. I., Neumann, A. L., and Mangual, R. S., "Energy and carbon emission savings in Spanish housing air-conditioning

using solar driven absorption system", ***Applied Thermal Engineering***, 28 (14–15): 1734–1744 (2008).

59. Dawahdeh, A. I. and Al-Nimr, M. A., "Energy and exergy analysis for a novel modified absorption Carnot battery", ***Journal Of Energy Storage***, 114: 115779 (2025).

60. Alfaris, A., Akroot, A., and Deniz, E., "The Exergo-Economic and Environmental Evaluation of a Hybrid Solar–Natural Gas Power System in Kirkuk", ***Applied Sciences***, 14 (22): 10113 (2024).

61. Lu, F., Zhu, Y., Pan, M., Li, C., Yin, J., and Huang, F., "Thermodynamic, economic, and environmental analysis of new combined power and space cooling system for waste heat recovery in waste-to-energy plant", ***Energy Conversion And Management***, 226: 113511 (2020).

62. Talal, W. and Akroot, A., "Exergoeconomic Analysis of an Integrated Solar Combined Cycle in the Al-Qayara Power Plant in Iraq", ***Processes***, 11 (3): (2023).

63. Ogaili, H. H., Khalilarya, S., Chitsaz, A., and Mojaver, P., "Energy, exergy, and economic performance analysis of integrated parabolic trough collector with organic rankine cycle and ejector refrigeration cycle", ***Energy Conversion And Management: X***, 25: 100843 (2025).

64. Mousavi Rabeti, S. A., Khoshgoftar Manesh, M. H., and Amidpour, M., "Techno-economic and environmental assessment of a novel polygeneration system based on integration of biomass air-steam gasification and solar parabolic trough collector", ***Sustainable Energy Technologies And Assessments***, 56: 103030 (2023).

65. Alperen, M. A., Kayabaşi, E., and Kurt, H., "Detailed comparison of the methods used in the heat transfer coefficient and pressure loss calculation of shell side of shell and tube heat exchangers with the experimental results", ***Energy Sources, Part A: Recovery, Utilization, And Environmental Effects***, 45 (2): 5661–5680 (2023).

66. Elmorsy, L., Morosuk, T., and Tsatsaronis, G., "Exergy-based analysis and optimization of an integrated solar combined-cycle power plant", ***Entropy***, 22 (6): 1–20 (2020).

67. Besevli, B., Kayabasi, E., Akroot, A., Talal, W., Alfaris, A., Assaf, Y. H., Nawaf, M. Y., Bdaiwi, M., and Khudhur, J., "Technoeconomic Analysis of Oxygen-Supported Combined Systems for Recovering Waste Heat in an Iron-Steel Facility", ***Applied Sciences***, 14 (6): 2563 (2024).

68. Wang, J., Lu, Z., Li, M., Lior, N., and Li, W., "Energy, exergy, exergoeconomic and environmental (4E) analysis of a distributed generation solar-assisted CCHP (combined cooling, heating and power) gas turbine system", ***Energy***, 175: 1246–1258 (2019).

69. Akroot, A., "Thermodynamic and Environmental Performance Analysis of the Marib Integrated Power and Cooling Cycle (MIPCC)", ***Black Sea Journal Of Engineering And Science***, 8 (3): 814–823 .

70. Nourpour, M., Khoshgoftar Manesh, M. H., Pirozfar, A., and Delpisheh, M., "Exergy, Exergoeconomic, Exergoenvironmental, Emergy-based Assessment and Advanced Exergy-based Analysis of an Integrated Solar Combined Cycle Power Plant", ***Energy And Environment***, 34 (2): 379–406 (2023).

71. Balghouthi, M., Chahbani, M. H., and Guizani, A., "Feasibility of solar absorption air conditioning in Tunisia", ***Building And Environment***, 43 (9): 1459–1470 (2008).

RESUME

Jamal Basheer Muhammad ALBARTOULI he studied at the Faculty of Engineering Technology in Benghazi. He is doing his master's degree at Karabük University, Faculty of Mechanical Engineering.